Theses and Dissertations — 1. Thesis and Dissertation Collection, all items

2009-12

Development of a laminar flame test facility for bio-diesel characterization

Tan, Giam

Monterey, California. Naval Postgraduate School

https://hdl.handle.net/10945/4338

NAVAL POSTGRADUATE SCHOOL

MONTEREY, CALIFORNIA

THESIS

DEVELOPMENT OF A LAMINAR FLAME TEST FACILITY FOR BIO-DIESEL CHARACTERIZATION

by

Giam Tan

December 2009

Thesis Advisor:	Jose O. Sinibaldi
Co-Advisor:	Knox T. Millsaps

Approved for public release; distribution is unlimited

THIS PAGE INTENTIONALLY LEFT BLANK

REPORT DOCUMENTATION PAGE		*Form Approved OMB No. 0704-0188*

1. AGENCY USE ONLY *(Leave blank)*	**2. REPORT DATE** December 2009	**3. REPORT TYPE AND DATES COVERED** Master's Thesis

4. TITLE AND SUBTITLE Development of a Laminar Flame Test Facility for Bio-Diesel Characterization	**5. FUNDING NUMBERS**
6. AUTHOR(S) Giam Tan	

7. PERFORMING ORGANIZATION NAME(S) AND ADDRESS(ES) Naval Postgraduate School Monterey, CA 93943-5000	**8. PERFORMING ORGANIZATION REPORT NUMBER**

9. SPONSORING /MONITORING AGENCY NAME(S) AND ADDRESS(ES) N/A	**10. SPONSORING/MONITORING AGENCY REPORT NUMBER**

11. SUPPLEMENTARY NOTES The views expressed in this thesis are those of the author and do not reflect the official policy or position of the Department of Defense or the U.S. Government.

12a. DISTRIBUTION / AVAILABILITY STATEMENT Approved for public release; distribution is unlimited	**12b. DISTRIBUTION CODE**

13. ABSTRACT (maximum 200 words)

The thesis examines the current testing standards for diesel fuels and establishes the relevance of such testing standards to bio-derived diesel fuels. There is a need for more detailed kinetics information for bio-diesel fuels to allow exploration of issues in engine and fuel design. Flame studies can provide overall chemical kinetic information that is currently lacking in the literature for bio-diesel fuels. An experimental apparatus to measure laminar flame speeds was designed and implemented to convey overall chemical reaction rate information. This work addressed three major aspects of such design: combustion chamber, auxiliary systems (gases and fuel supply, ignition, and control) and measurement systems. Test rig characterization was attempted; however, critical ignition and fueling issues were uncovered during experimentation. Suggestions for future work provide solutions and improvement pathways to the current design.

14. SUBJECT TERMS Laminar Flame Speed Test, Test Faculty Characterization for Bio-Diesel Characterization, Combustion Chamber, Ignition, Fuelling.	**15. NUMBER OF PAGES** 87
	16. PRICE CODE

17. SECURITY CLASSIFICATION OF REPORT Unclassified	**18. SECURITY CLASSIFICATION OF THIS PAGE** Unclassified	**19. SECURITY CLASSIFICATION OF ABSTRACT** Unclassified	**20. LIMITATION OF ABSTRACT** UU

NSN 7540-01-280-5500

Standard Form 298 (Rev. 8-98)
Prescribed by ANSI Std. Z39.18

i

THIS PAGE INTENTIONALLY LEFT BLANK

DEVELOPMENT OF A LAMINAR FLAME TEST FACILITY FOR BIO-DIESEL CHARACTERIZATION

Giam Tan
Major, Republic of Singapore Air Force
B.S., Nanyang Technological University, 1998

Submitted in partial fulfillment of the
requirements for the degree of

MASTER OF SCIENCE IN MECHANICAL ENGINEERING

from the

NAVAL POSTGRADUATE SCHOOL
December 2009

Author: Giam Tan

Approved by: Jose O. Sinibaldi
                 Thesis Advisor

                 Knox T. Millsaps
                 Co-Advisor

                 Knox T. Millsaps
                 Chairman, Department of Mechanical and Astronautical
                 Engineering

iii

THIS PAGE INTENTIONALLY LEFT BLANK

ABSTRACT

The thesis examines the current testing standards for diesel fuels and establishes the relevance of such testing standards to bio-derived diesel fuels. There is a need for more detailed kinetics information for bio-diesel fuels to allow exploration of issues in engine and fuel design. Flame studies can provide overall chemical kinetic information that is currently lacking in the literature for bio-diesel fuels. An experimental apparatus to measure laminar flame speeds was designed and implemented to convey overall chemical reaction rate information. This work addressed three major aspects of such design: combustion chamber, auxiliary systems (gases and fuel supply, ignition, and control) and measurement systems. Test rig characterization was attempted; however, critical ignition and fueling issues were uncovered during experimentation. Suggestions for future work provide solutions and improvement pathways to the current design.

THIS PAGE INTENTIONALLY LEFT BLANK

TABLE OF CONTENTS

LIST OF FIGURES

LIST OF TABLES

THIS PAGE INTENTIONALLY LEFT BLANK

ACKNOWLEDGMENTS

THIS PAGE INTENTIONALLY LEFT BLANK

I.   INTRODUCTION

A.   MOTIVATION

The current testing standards for liquid fuels and the relevance of such testing standards were evaluated and applied to bio-diesel fuels. To allow exploration of issues in engine and fuel design, there is, however, a need for more detailed kinetics information for bio-diesel fuel. To understand the impact of fundamental combustion properties, such as ignition characteristics, laminar flame speed, strain sensitivity and extinction strain rates on emission and stability characteristics of Diesel engines and their operation with bio-diesel fuels, extensive research is ongoing [1].

Many simplified models are used to predict the static stability of the combustor heavily rely on laminar flame speed information. This is because it has a significant impact upon the propensity of a flame to flashback and blow off [2]. In addition, it serves as a key scaling parameter for other important combustion characteristics, such as the turbulent flame structure, turbulent flame speed and flame's spatial distribution [3]. Therefore, the vision is that further flame studies will provide important kinetics validation data for bio-diesel-like fuels. This motivated the design for a vertical combustion chamber to measure flame speeds of the varying strains of bio-diesel fuels. This key parameter contains fundamental information regarding reactivity, diffusivity, and exothermicity of the fuel mixture [4].

The flame experiments are challenging: the tested bio-fuel must be uniformly atomized and uniformly dispersed. The current test rig was developed with provisions for optical access and for future spectroscopic measurements.

1

B. THE PRINCIPLE OF LAMINAR FLAME SPEED

Laminar flame speed contains fundamental information regarding reactivity, diffusivity, and exothermicity of the fuel mixture. It serves as a good validation parameter for leading kinetic models used for detailed combustion simulations [5]. The former also serves in the prediction of static stability of combustors. This is because it has significant impact upon the propensity of a flame to flashback and blow off [6].

Laminar flame speed can be defined as the velocity that a planar flame front travels relative to the unburned gas in a direction normal to the flame surface [7]. From a simplified analysis of a flame, based on a balance between heat release and diffusion, the laminar flame speed, S_L can be modelled as

$$S_L \approx \sqrt{\frac{\alpha \times RR}{\rho}}$$

where α is the thermal diffusivity, RR is the overall reaction rate, and ρ is the unburned gas density. To calculate the laminar flame speed, the thermo physical properties of the fuel mixture at high temperatures must be determined to have a more accurate reaction rate [8, 9]. This data, however, is not available for many fuels and even less so for bio-diesel fuels. Therefore, a direct experimental measurement is warranted.

C. FACTORS AFFECTING LAMINAR FLAME SPEED

There are four main factors that can directly or indirectly effect and influence laminar flame speed. They are: pressure, pre-heat temperature, hydrogen to carbon ratio (H to C ratio) of the fuel as well as the effect of dilution [10, 11].

1. **Pressure**

An increase in pressure is expected to increase the overall reaction rate (*RR*) and, hence, increase the laminar flame speed according to the proposed model. On the other hand, the increased density of the reactant mixture with increase in pressure necessitates more thermal energy transfer from the reaction zone to raise the reactant temperature in the preheat zone. Since diffusivity is also inversely proportional to pressure, the overall increase in pressure increases flame speed.

2. **Pre-Heat Temperature**

The preheat temperature influences the laminar flame speed mainly through the changes in reaction rate and diffusive properties. An increase in preheat temperature also increases the adiabatic flame temperature. It is also known that the rate of increase is more for lean mixtures than for stoichiometric or rich mixtures.

3. **Hydrogen to Carbon Ratio**

Flame speed increases as the relative amount of H in the fuel increases. This behaviour can be explained by the fact that the overall reactivity of the fuel mixture increases with the amount of H as the low molecular weight of hydrogen acts to increase the diffusivity of the reactant mixture.

4. **Diluents**

The presence of diluents in the fuel, such as CO_2, N_2 and H_2O, will reduce the flame temperature and, thus, reduce the laminar flame speed through a reduction in overall reaction rate. The diluents are not inert and can potentially impede flame propagation. The diluents present in the fuel can also influence flame propagation through radiative heat transfer. Most diluents are effective absorbers and emitters of infrared radiation and will result in absorption of energy

radiated from the hot products This enhancement of thermal energy transfer across the flame aids in flame propagation and, hence, increases the laminar flame speed.

D. NATURE OF BIO-FUEL

Bio-diesel is a promising alternative to petroleum-based diesel fuels. This is because it is a renewable energy source and provides an avenue for the DoD to become energy-independent from rogue nations' oil supplies [12]. Its extensive use in unmodified engines has proved to be very successful. Agricultural fat and oils, in raw or chemically modified forms, have the potential to supplant a significant proportion of petroleum-based fuels [13]. Bio-diesel is of particular interest to the automobile industry, and other areas in energy and the environment, because it significantly reduces particulate matter (PM), hydrocarbon (HC) and carbon monoxide (CO) emissions and the net production of carbon dioxide (CO_2) from combustion sources (note that no modifications to the engines are necessary [14]. Bio-diesel is also the only alternative fuel that has passed the Environmental Protection Agency (EPA)-required Tier I and Tier II Health Effects testing requirements of the Clean Air Act Amendments of 1990[1]. In addition, bio-diesel is particularly attractive because it is a renewable fuel that can be replenished through the growth of plants or algae or production of livestock. It has the potential to supplant a fraction of petroleum-based fuels.

Depending on the quality of the bio-extender, biofuels can have different characteristics from conventional refined fuels: they may potentially polymerize with heat. Therefore, testing of both bio-diesel-extender and finished blends is important [15]. Testing helps to protect engines and fuel pumps from potential

---

[1] Extracted from: www.biodiesel.org.au. Accessed 15 July 2009.

damage and deposits caused by poor stability, organic insoluble matter, water and contamination from metals or bi products from the trans-esterification process[2].

Bio-diesel and bio-ethanol are the two main bio-fuels. The two groups of bio-fuels are: first generation bio-fuels made from a food source; second generation bio-fuels involve crops not used primarily as a food source [16].

There are several problems with bio-fuels: they cost more than fossil fuels [17]. Many bio-fuels are first generation. This has effected food supply and caused food prices to increase. Our dependence on the crops for food also limits production growth. Bio-fuels are in small-scale production, but it is difficult making production large enough to supply enough fuel to replace fossil fuels[3].

E.   CURRENT TESTING STANDARD FOR BIO-FUEL

Oil companies and vehicle manufacturers are actively working with biofuel extender producers to obtain agreement on the standards for trans-esterified vegetable oils suitable for blending with conventional diesel. This is to ensure that the product meets the technical requirements of modern diesel engines [18]. The minimum test requirements for biodiesel blend extenders are specified in ASTM D6751[4] in USA and EN 14214[5] within Europe.

To maintain standards, it is vital that all road fuels are subject to strict quality controls. In addition, it is important to provide authorities with the ability to

---

[2] Trans-esterification is defined as a chemical process involving the exchange of organic group R'' of an ester with the organic group R' of an alcohol and often catalyzed by the addition of an acid or base.

[3] Extracted from: www.alternative-energy-news.info/biofuels-alternative-fossil-fuels. Accessed 17 July 2009.

[4] ASTM D6751-08 details standards and specifications for bio-diesels blended with middle distillate fuels. This specification standard specifies various test methods to be used in the determination of certain properties for bio-diesel blends and kinematic viscosity.

[5] EN 14214 is an international standard that describes the minimum requirements for bio-diesel. The European Standard was approved by CEN (European Committee for Standardization).

assess safety risks and environmental pollution [19]. For example, regular mineral diesel is subject to the EN 590 standard. In 1997, the European Committee for Standardization was given the task to develop a uniform standard for Fatty Acid Methyl Ester (FAME). The result was the EN 14214 specification. The introduction of this standard in 2004 is valid for all member states of the European Union [20]. In particular, this standard gives engine and automobile makers the ability to give warranties to those vehicles that run on bio-diesel. At present a limit of 5% FAME is allowed in EN 590[6] diesel. This 5% must conform to the EN14214 standard. Table 1 depicts the various testing standards for bio-diesel.

---

[6] EN 590 describes the physical properties that all automotive diesel fuels must meet if they are to be sold in the European Union, Iceland, Norway and Switzerland.

Bio-diesel Standards	Unit	EN 14214	ASTM D 6751	EN 590
Density 15°C	g/cm³	0.86-0.90	-	0.82-0.845
Viscosity 40°C	mm²/s	3.5-5.0	1.9-6.0	2.0-4.5
Distillation	% @ °C	-	90%,360°C	85%,350°C - 95%,360°C
Flashpoint (Fp)	°C	101 min	93 min	55 min
Sulphur	mg/kg	10 max	15 max	350 max
CCR 100%	%mass	-	0.05 max	-
Carbon residue (10%dist.residue)	%mass	0.3 max	-	0.3 max
Sulphated ash	%mass	0.02 max	0.02 max	-
Oxid ash	%mass	-	-	0.1 max
Water	mg/kg	500 max	500 max	200 max
Total contamination	mg/kg	24 max	-	24 max
Cu corrosion max	3h/50°C	1	3	1
Oxidation stability	hrs;110°C	6 hours min	3 hours min	N/A (25 g/m3)
Cetane number		51 min	47 min	51 min
Acid value	mgKOH /g	0.5 max	0.5 max	-
Methanol	%mass	0.20 max	0.2 max or Fp <130°C	-
Phosphorus	mg/kg	4 max	10 max	-
Gp I metals (Na,K)	mg/kg	5 max	5 max	-
GpII metals (Ca,Mg)	mg/kg	5 max	5 max	-
Triglyceride	%mass	0.2 max	-	-
Free glycerol	%mass	0.02 max	0.02 max	-
Bio-diesel Standards	Unit	EN 14214	ASTM D 6751	EN 590
Total glycerol	%mass	0.25 max	0.24 max	-
Ester content	%mass	96.5 min	-	-

Table 1.   Testing Standards for Bio-Diesel (Extracted from Biofuel Systems Group: www.biofuelsystems.com/biodiesel/specification. Accessed 19 Aug 2009.)

The current established and widely used testing standards[7] for bio-fuel are depicted as follows:

1.   Density (EN ISO 3675, EN ISO 12185)

Bio-diesels generally have higher densities than mineral diesel (EN 590 820-845 kg/m^3 at 15°C). Density increases with a decrease in chain length and with unsaturation. This can have an impact on fuel consumption. This is because the fuel introduced into the combustion chamber is determined volumetrically.

2.   Viscosity (EN ISO 3104, ISO 3105, D445)

Viscosities of neat vegetable oils are many times higher. This leads to serious problems in unmodified engines. The increase in viscosity results in poor atomization and incomplete combustion. The latter leads to coking of injector tips. This results in engine power loss. Bio-diesel still has higher viscosity than mineral diesel (3.50-5.00 mm^2/s at 40°C vs. 2.00-4.50 mm^2/s). Viscosity decreases with unsaturation, but increases markedly with contamination by mono, di or tri glycerides.

3.   Flash Point (ISO 3679, IP 523, IP 524, D93)

Pure rapeseed methyl ester has a flash point value of up to 170°C. This method is, therefore, looks at residual components within the fuel that are combustible, especially methanol that is a particular hazard due to its invisible flame.

4.   Sulphur Content (EN ISO 20846, EN ISO 20884, D5453)

Sulphur emissions are harmful to human health. In addition, high sulphur fuels cause greater engine wear and, in particular, shorten the life of the catalyst. Bio-diesel derived from pure rapeseed oil will contain virtually no sulphur. FAME derived from animal sources, however, may contain significant quantities.

---

[7] Extracted from source: www.biofuelstesting.com/quality_control.asp. Accessed 10 July 2009.

5.   Carbon Residue (EN ISO 10370)

The Carbon Residue is the material left after evaporation and pyrolysis of a sample fuel. This is a measure of the tendency of a fuel to produce deposits on injector tips and the combustion chamber. For FAME samples, it is an indication of the amount of glycerides, free fatty acids, soaps and catalyst residues remaining within the sample.

6.   Cetane Number (EN ISO 5165, D613)

This serves as a measure of ignition quality. This is the most pronounced change from vegetable oil to the transesterified product. Due to incomplete combustion, fuels with low cetane numbers show an increase in emissions. Palm Oil and Tallow-derived bio-diesels have the best cetane numbers.

7.   Sulphated Ash (ISO 3987, D874)

Ash describes the amount of inorganic contaminants, such as catalyst residues, remaining within the fuel. Ash relates to engine deposits on combustion.

8.   Water Content (EN ISO 12937)

As FAME is hygroscopic, it can pick up water in storage. As such, there can be problems meeting the specification. At around 1500 ppm, the solubility limit is reached and the water bottoms out. Free water promotes biological growth and the reverse reaction turns bio-diesel into free fatty acids.

9.   Total Contamination (EN 12662)

The definition of total contamination is the insoluble material retained after the filtration of a heated sample over a standardized 0.8mm filter. FAME samples with high quantities of insoluble materials tend to cause fuel filter and injector blockages. High concentrations of soap stock are normally associated with high total contamination.

10.   Copper Strip Corrosion (EN ISO 2160, D130)

This is defined as the likelihood to cause corrosion to copper, zinc and bronze parts of an engine. Heat a polished metallic strip at 50°C for 3 hours and, then, washed and compared to standards. Free acids or sulfur compounds likely cause corrosion. FAME, however, gives consistently good results in this area and is unlikely to fail due to low sulfur content.

11.   Oxidation Stability (EN 14112)

The Oxidative stability specification is defined as a minimum Rancimat induction period of six hours. Essentially a fuel heats at 110°C in a constant air stream and the formation of volatile organic acids is detected. This property relates to the overall storage stability of the fuel. The higher the degree of unsaturation (double bonds) within the FAME molecules equates to a decrease in oxidative stability. The addition of antioxidant additives can improve this.

12.   Acid Value (EN 14104, D664)

Acid value is a measure of mineral acids and free fatty acids contained in a fuel sample. It is expressed in mg KOH required to neutralize 1g of FAME. High fuel acidity is linked with corrosion and engine deposits.

13. Iodine Value (EN 14111)

Iodine number is a measure of total unsaturation (double bonds) within the FAME product. It is expressed as the grams Iodine requires to react with 100g of FAME sample. High Iodine value relates to polymerization of fuels, which leads to injector fouling. It is also linked to poor storage stability.

14. Ester Content (EN 14103)

This is measured using gas chromatography and is restricted to esters falling within the C_{14}-C_{24} range. It is ultimately a test for reaction conversion. As linolenic and polyunsaturated esters have been shown to display a disproportionately strong effect on oxidative stability, they are controlled.

15. Methanol Content (EN 14110)

Methanol can be removed from FAME by washing or distilling. Due to the very low flash point of methanol, high methanol contents pose safety risks.

16. Glycerides (EN 14105, EN 14106, D6584)

There is a limit on the mono, di, and triglycerides of no more than 0.80%, 0.20% and 0.20% respectively. Total glycerol is the sum of the bound and free glycerol and must not exceed 0.25%/. Failing to meet the specification implies low conversion to ester and deposit formation on injectors and valves.

17. Group I Metals

Sodium and Potassium are limited to a combined 5ppm. These arise from the addition of catalyst and result in high ash levels in the engine.

18.   Group II Metals

Calcium and Magnesium are limited to a combined 5ppm. These may rise from the addition of hard water in the washing process. Calcium and Magnesium soaps have been related to injector pump sticking.

19.   Phosphorous Content (EN14107, D4951)

The phosphorous limit is approx 10 ppm and normally rises from phospholipids within the starting material or from the addition of phosphoric acid in the production process. High phosphorus fuels are suspected of poisoning catalysts and increasing emissions.

20.   CFPP (EN 116)

Cold-Filter Plugging Point is considered a suitable indicator of low temperature operability. It defines a temperature at which a fuel is no longer filterable within a specified time limit.

II.   FLAME-SPEED EXPERIMENTATION

A.   TESTING METHODOLOGY

The objective of this thesis is to design and build a laboratory-based flame speed test rig for the measurement of laminar flame speeds of fuel-air and bio-fuel air mixtures at standard conditions.

A premixed charge is prepared by adding the required amount of fuel to a controlled quantity of air. The desired amount of liquid fuel is delivered by means of a fuel injector whose flow rate varies linearly with fuel pressure. The flow rates of air are controlled using calibrated choked orifices. Thus, by setting the upstream pressures, the flow rates can be controlled. The liquid fuel is atomized into fine droplets using an ACDelco fuel injector originally designed for service in direct fuel injected engines.

The injector operates with fuel pressures ranging from 50 to 2500 psi. The large pressures are used to atomize the fuel into droplets with Sauter mean diameters (D_{32}) between 5 and 15 μm. Residence time in the combustion chamber allows for vaporization of such droplets following a D_2 law.

The almost quiescent fuel-air mixtures are consequently ignited by a spark discharge inside a combustion chamber. A spherically expanding flame kernel should develop until the flame reaches the walls where a laminar flame should start to propagate into the unburned reactants.

Optical measurements using the Thorlabs DET36A detectors installed along the combustor walls provide the time-of-arrival (TOA) measurements. From this we can determine the flame speed by dividing the distance between detectors by the difference in TOA. Data is recorded on a Tektronix DPO4104 Oscilloscope.

B. EXPERIMENTAL TEST MATRIX

Due to kerosene fuel availability, it will be used to characterize the test rig. The laminar flame speeds of these kerosene-air mixtures are experimentally measured. The flame speed data are obtained for a range of equivalence ratios from 0.8 to 1.4.

C. EXPERIMENTAL SET-UP

The experimental test rig comprises of four main modules: a) combustion chamber, b) exhaust system, c) control system and d) the supply system. The selection criteria for the material and component, as well as the embedded design considerations for the respective modules, are elaborated in this section.

1. The Combustion Chamber

The combustion chamber (Figure 1) consists of three stainless steel pipes attached and pressure-sealed. Due to its chemical inertness and structural rigidity, stainless steel is selected for the fabrication of the combustion chamber. It was installed in a vertical orientation. To attain pressure-sealed conditions for the chamber, gaskets are placed between the interfaces of the flanges. Along each side of the pipe are national pipe thread (NPT) threaded holes meant for attaching optical sensors and other measuring instruments (refer to Figure 2). Standard NPT connectors and Swagelok fittings and stainless steel tubing are used for the auxiliary systems to the combustion chamber.

Figure 1.   The Combustion Chamber
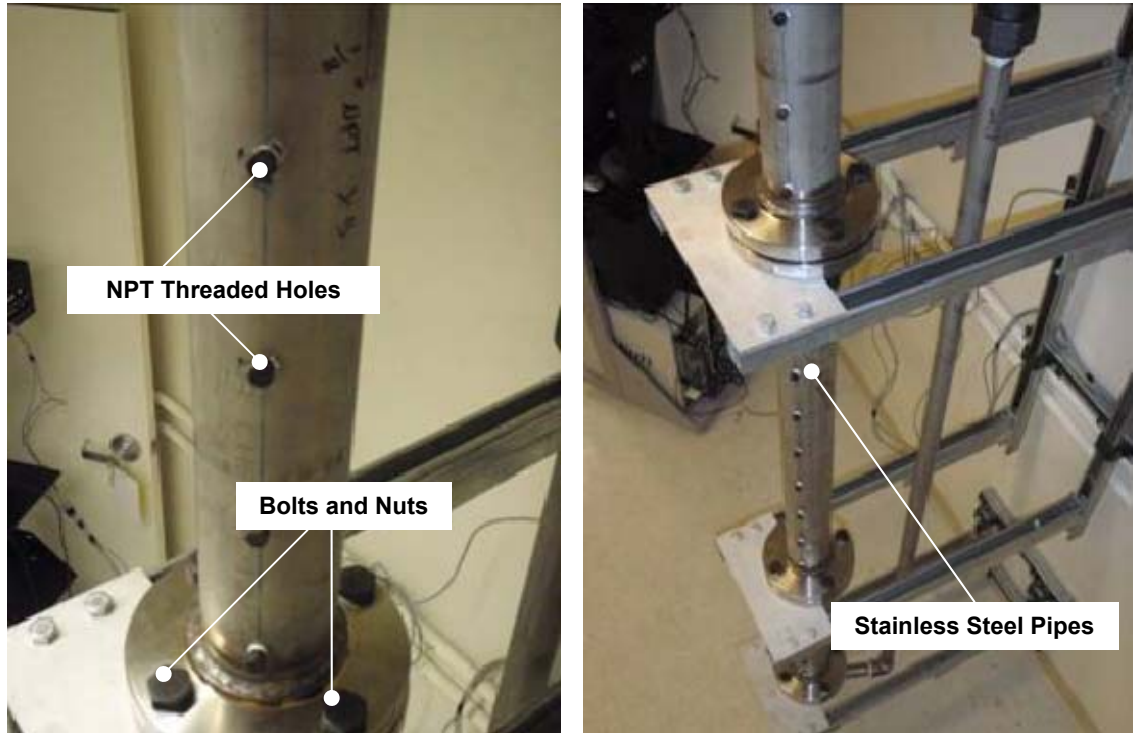
Figure 2.   Combustion Chamber with NPT Threaded Holes for
Instrumentation

a.   *Fuel Injector*

The top flange of the combustion chamber (depicted in Figure 3) has inlet ports for nitrogen, pressurized air, and outlets to the exhaust system. To have better fuel-air mixing as air flows into the combustion chamber, the inlet ports are chamfered on the inward side. The piping inlets surround a housing attachment for a fuel injector located at the center of the top flange. The fuel Injector (ACDelco ACD217-3086) is depicted in Figure 4. The housing attachment connects directly to a fuel piping, where it will collect the fuel and nozzle-spray into the combustion chamber for mixing with the air (refer to Figure 5). The fuel injector housing attachment was designed and fabricated from Aluminum 6061-T6. Aluminum was selected because of its high thermal conductivity. This enables better dissipation of heat from the fuel injector during operation.
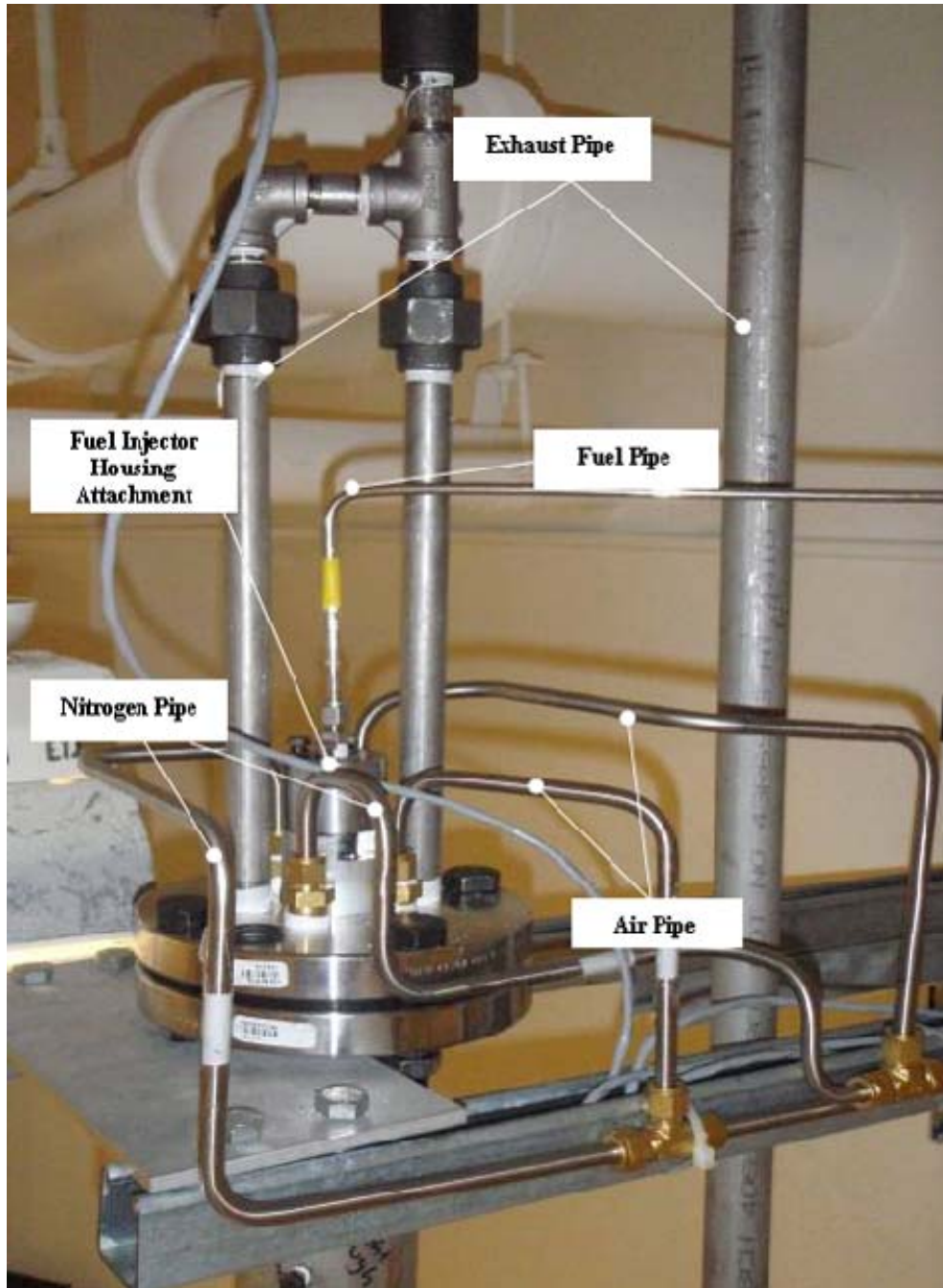
Figure 3.   Top Flange of the Combustion Chamber with Inlets for
Nitrogen, Pressurized Air, Outlets to Exhaust System and Fuel Injector
Housing

Figure 4.   Fuel Injector
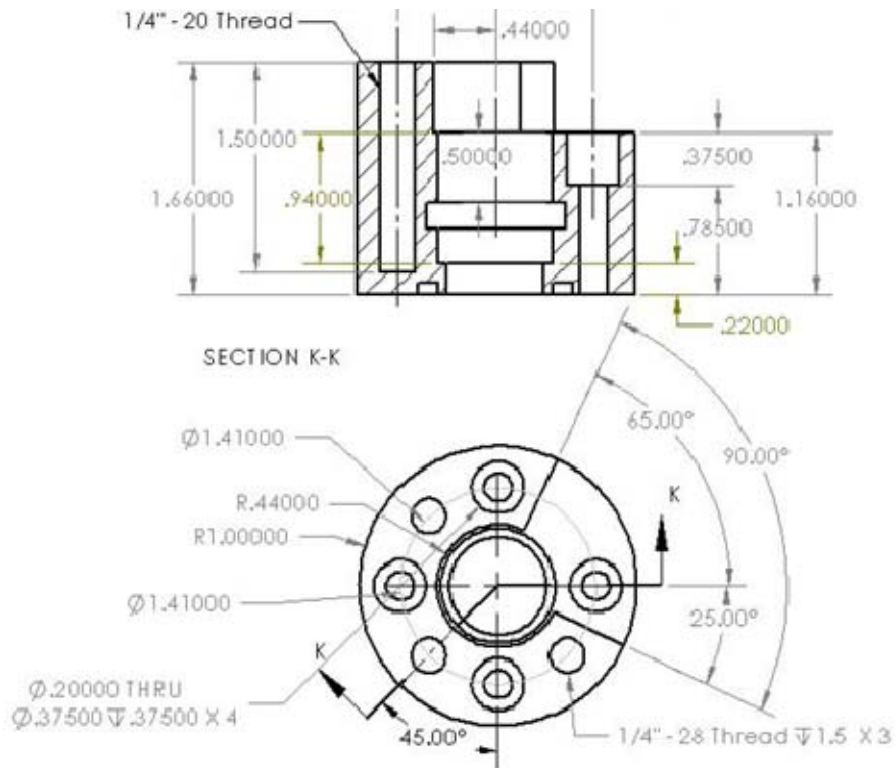
Figure 5.   Housing Attachment for Fuel Injector
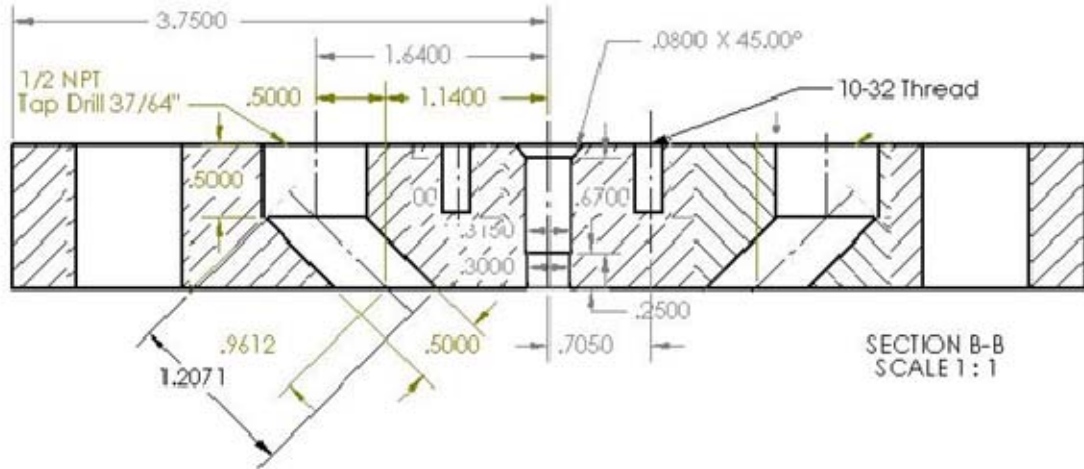
Figure 6.   Cross-sectional View of Flange

A Swagelock 7 μm fuel filter (Figure 7) is also connected before the fuel line enters the fuel injector. The function of the fuel filter is to prevent debris in the fuel from damaging the fuel injector.
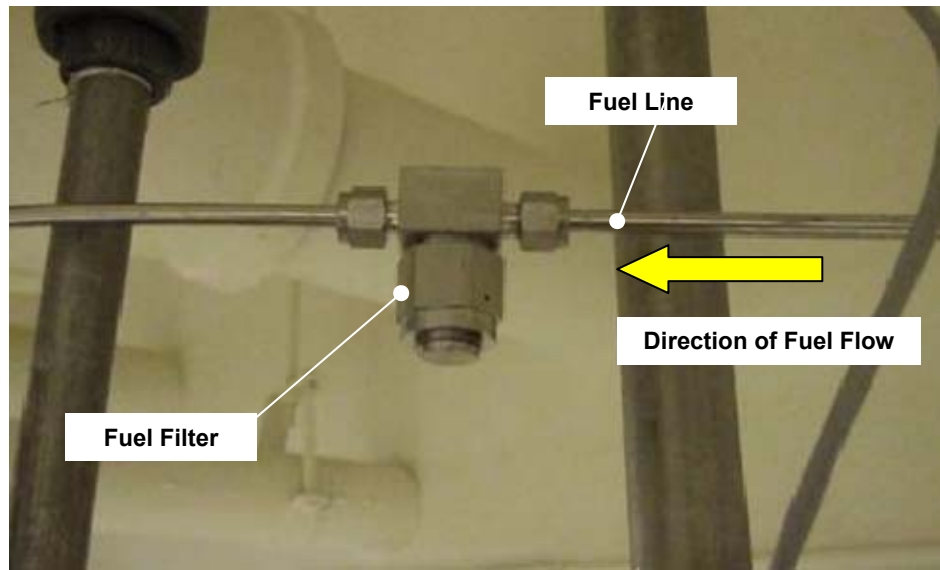
Figure 7.   Fuel Filter (7 μm) Installation

The fuel injector is selected based on research that it is able to generate droplets of fuel with Sauter mean diameters (D_{32}) between 5 and 15 μm. This is based on the D^2 law computation and assumes that a single kerosene droplet in a quiescent (non-convective) atmosphere at standard condition. The evaporation time[8] (t_v) for the fuel droplet can be denoted as

$$d^2 = d_0{}^2 - \left[\frac{8 \times \rho_s \times \alpha_s \times \ln(1+B)}{\rho_l} \right] \times t_v$$

where density of liquid kerosene (ρ_l) = 817 kg/m^3

density of vapour kerosene (ρ_s) = 5.418 kg/m^3

diffusivity for kerosene (α_s) = 0.0206 μm^2/s

transfer number for kerosene (B) = 3.4

As stipulated in Figure 8, the square of kerosene droplet diameter (d^2) is plotted against the evaporation time (t_v). The plot also clearly demonstrates the effect of pre-heating the fuel before pumping to the fuel injector. At 800K, for the same droplet diameter of 40 μm, increasing the temperature of fuel reduces the density of the liquid kerosene and reduces the evaporation time.

---

[8] Equation and parameters are referenced from Kenneth K. Kuo, Principles of Combustions, 2005, 236-257.
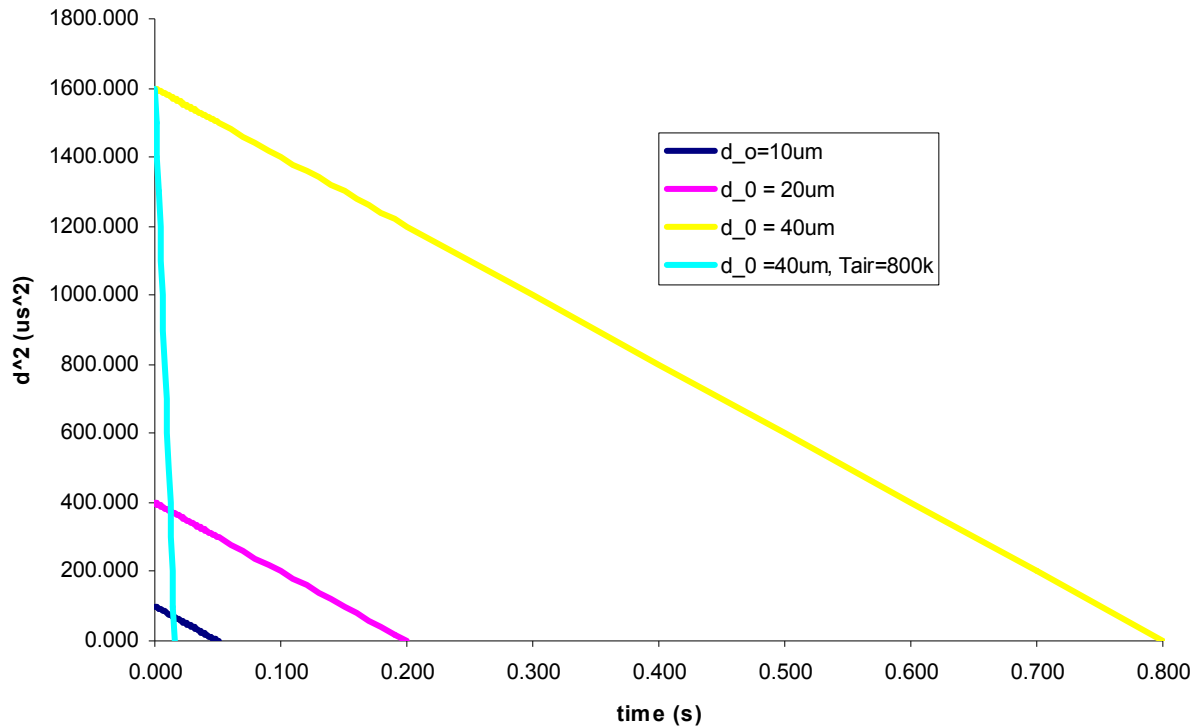
Figure 8.　　　　　Kerosene Droplet Evaporation based on D^2 Law

To ensure homogenous mixing of fuel and air in the combustor before ignition can take place, it is crucial to achieve short evaporation time (typically < 1 sec). It is noted that the turbulence decay is approximately about 30 sec under similar testing conditions for the design test rig. It is also important for the fuel droplets to be able to evaporate fast so that the laminar condition can still be attained at the ignition point. The importance of sizing the appropriate fuel injector that is able to generate both uniform and small droplet diameter cannot be over emphasized.

21

b. High Speed Si Detector

During the experiments, high-Speed Si detectors (350-1100 nm, 14 ns rise time) are mounted in the equally spaced threaded holes to detect the passing flame wave and are mounted to the combustor as shown in Figure 9. With known separations between each threaded hole, as well as the time taken for the flame wave to pass from one detector to another, the speed of the flame can then be computed.
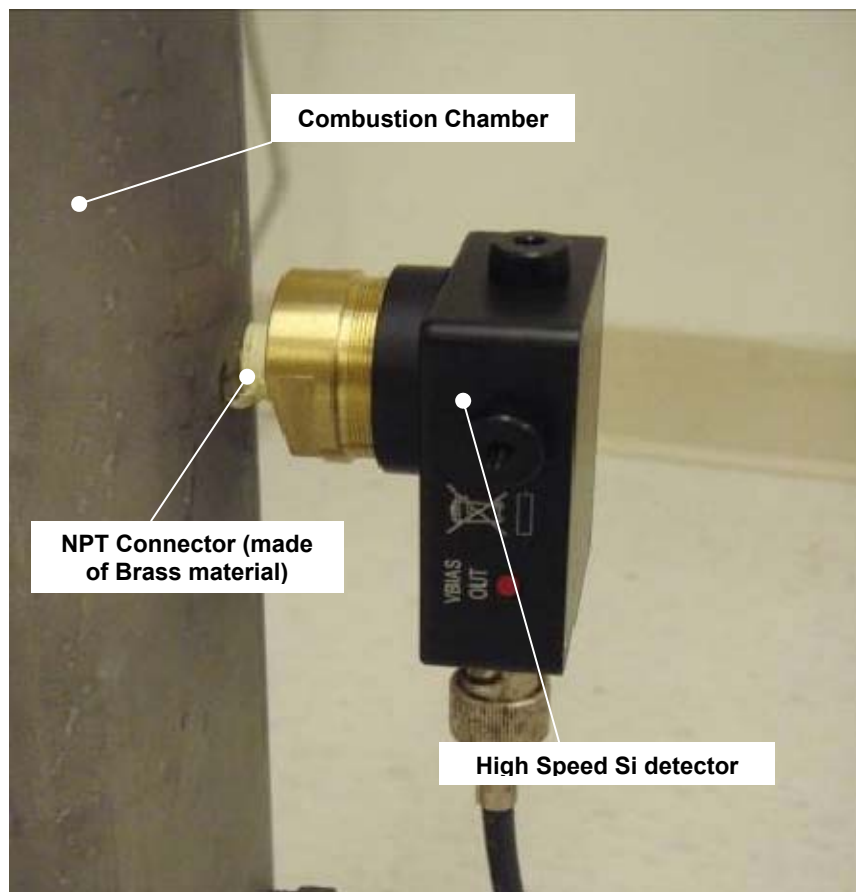
Figure 9.   Mounting of High Speed Detectors to Combustion Chamber

To provide the function of igniting the fuel and air mixture (depicted in Figure 10), the two tungsten electrodes extrude themselves into the combustion chamber, perpendicular from the threaded holes situated below the top flange. A Piezoelectric device (NJ 001A3), shown in Figure 11, is used to generate the required voltage across the tungsten electrodes. When the button of the device is pushed, a small spring-loaded hammer within the device hits the piezoelectric crystal. This generates high voltage across the face of the crystal. The voltage is relayed via conducting wire to the tungsten electrodes, creating sparks at the tip of the electrodes.
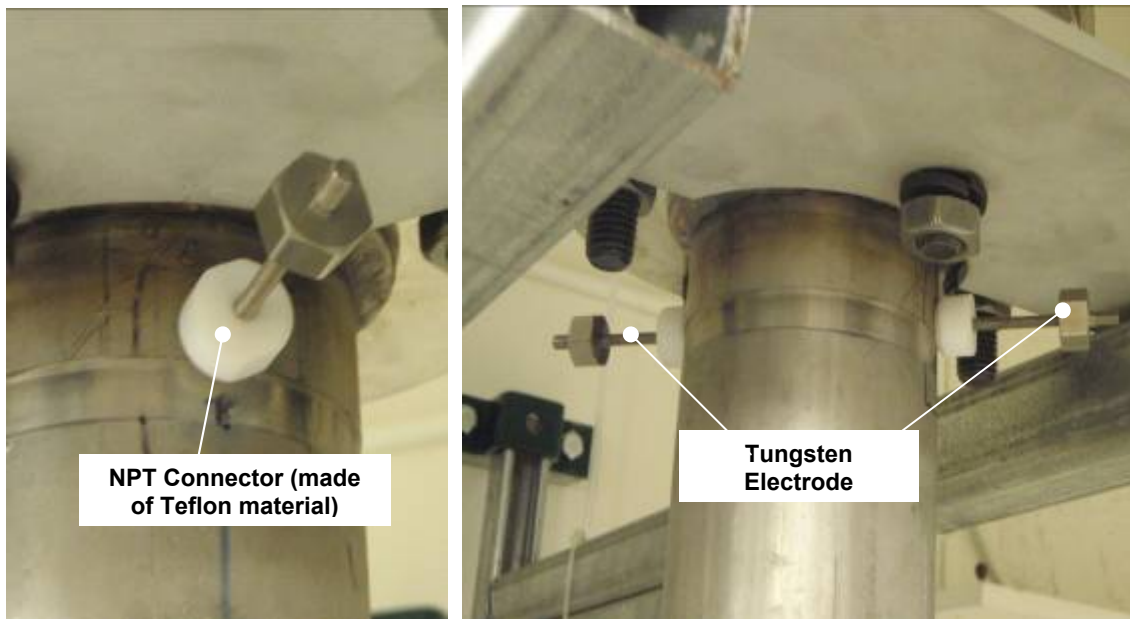
Figure 10.   Tungsten Electrodes Mounting on the Combustion Chamber

Figure 11.　　　　　　　Piezoelectric Igniter

The bottom section of the combustion chamber (refer to Figure 12) consists of an attachment of a manual hand valve that allows the flushing of the combustion chamber via the base of the combustion chamber. Horizontal and vertical structural beams (depicted in Figure 13) attached directly to the wall support the entire combustion chamber from the ground. For ease of assembly, these were made using the Unistrut system.

Figure 12.　　　　　　　Bottom View of Combustion Chamber
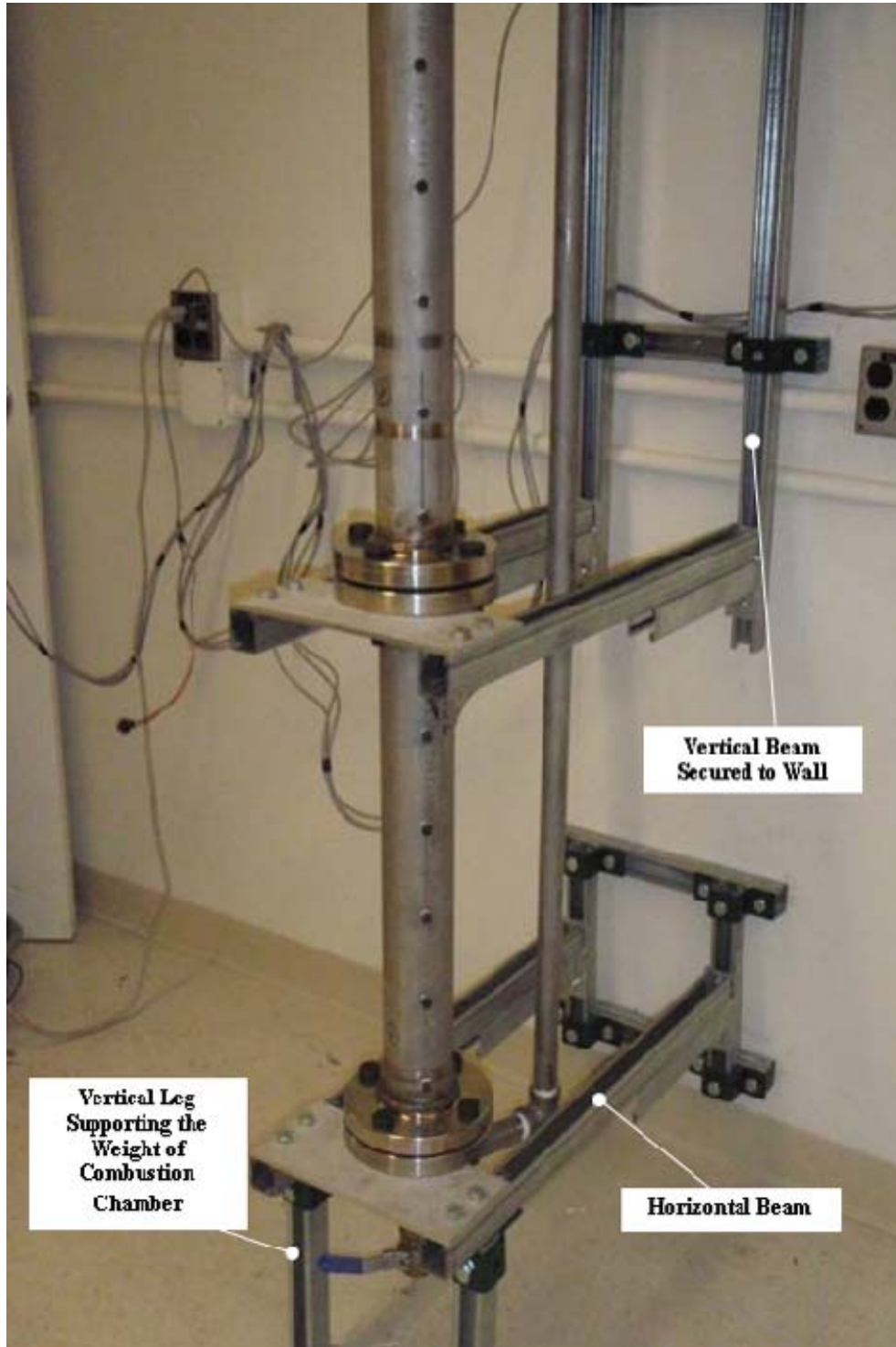
Figure 13.   Horizontal and Vertical Structural Beams

2. The Exhaust System

The exhaust system consists of a pneumatic ball valve (Gemini SM50-A512) at the top of the combustion chamber (Figure 14), as well as a manually operated flush valve found at the bottom of the combustion chamber (Figure 15). Because of the same considerations for the combustion chamber, the exhaust piping is also made from stainless steel.

Figure 14.   Exhaust System's Pneumatic Ball Valve

Figure 15.   Exhaust System's Flush Valve

To allow for remote operation of test rig, electro-pneumatic controlled ball valves are employed throughout the supply system. During the conduct of experiments, the hand valve at the bottom of the combustion chamber remains open to channel any un-burned fuel or air to flow to the exhaust system. An on/off switch connected to power relays controls the air-operated valve at the top of the combustor. To purge the combustion chamber and also to maintain a balanced pressurized condition within the combustion chamber during the experiments, the switch is opened when required.

3.   The Control System

The control system enclosure is depicted in Figure 16 and its internal components in Figure 17. These are comprised of a pulse generator, a series of solid-state relays, a 5VDC power supply and three 24VDC power supplies. The front panel of the enclosure has a series of lever switches that provide a 5VDC signal to the control logic side of the solid-state relays. These in turn send out the 24VDC power to the respective electro-pneumatic ball valves. The fuel injector lever sends a series of 5VDC pulses with a nominal 1ms duration on a 50% duty cycle to the solid-state relay which, in turn, sends similar 24VDC pulses to the fuel injector. The reason for this complex control logic is to prevent overheating of the fuel injector's coil. The control system also has a turning knob for setting the required frequency of the pulse generator.

The right-hand lever at the right of the panel serves as the main power activation lever. The LED indicates whether the control system is at the off/on position. Figure 15 depicts the internal circuitry of the control system.
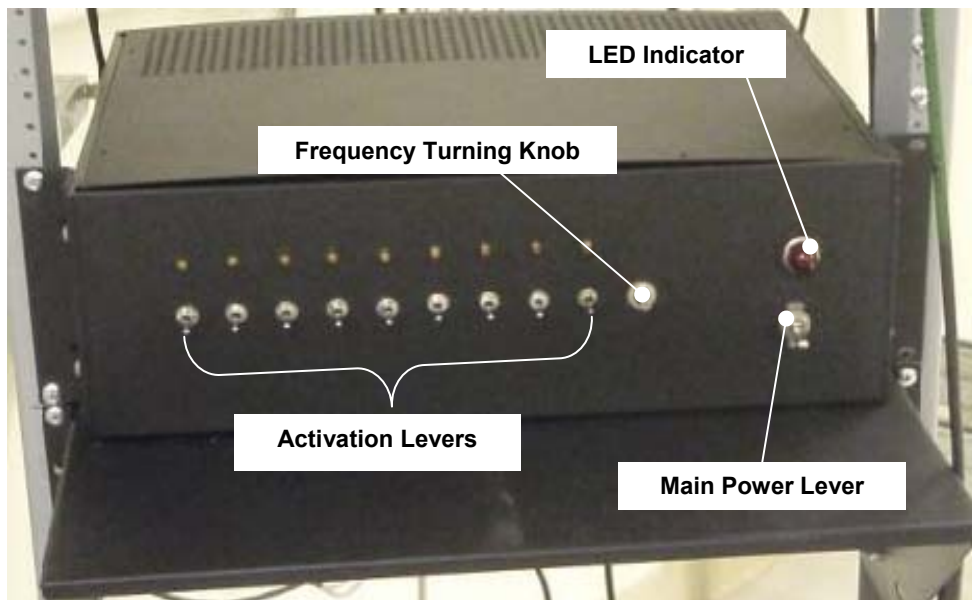
Figure 16.   Control System Enclosure
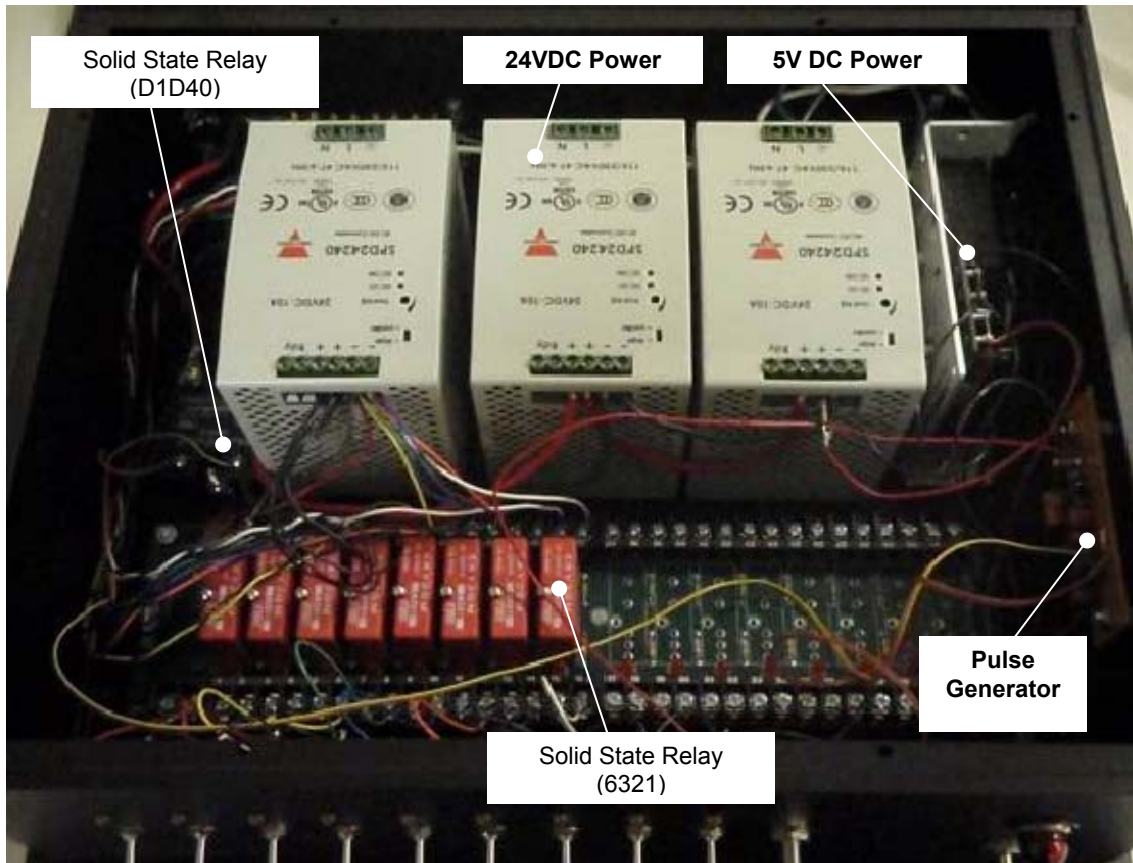
Figure 17.   Control System Internal Layout

The pulse generator (refer to Figure 18) is designed and placed in the control circuitry to control an output of 5V DC supply to the CRYDOM solid-state relay D1D40 (see Figure 19) over a range of duty cycle from 20.5 % to 42.3%. The pulse generator consists of a stable controller (FAIRCHILD Semiconductor NE555) capable of producing accurate timing pulses with adjustable duty cycle and high current drive capability connected to an Inverter (FAIRCHILD Semiconductor DM74LS14). The Inverter performs a logic Invert function and transforms a change input signal to a fast changing, jitter free output. The 5VDC pulsating output signal from the pulse generator enters the input of CRYDOM solid-state relay D1D40 and relays a pulsating output of 20VDC (from the 24V DC supplies) to the fuel injector based on the selected duty cycle.
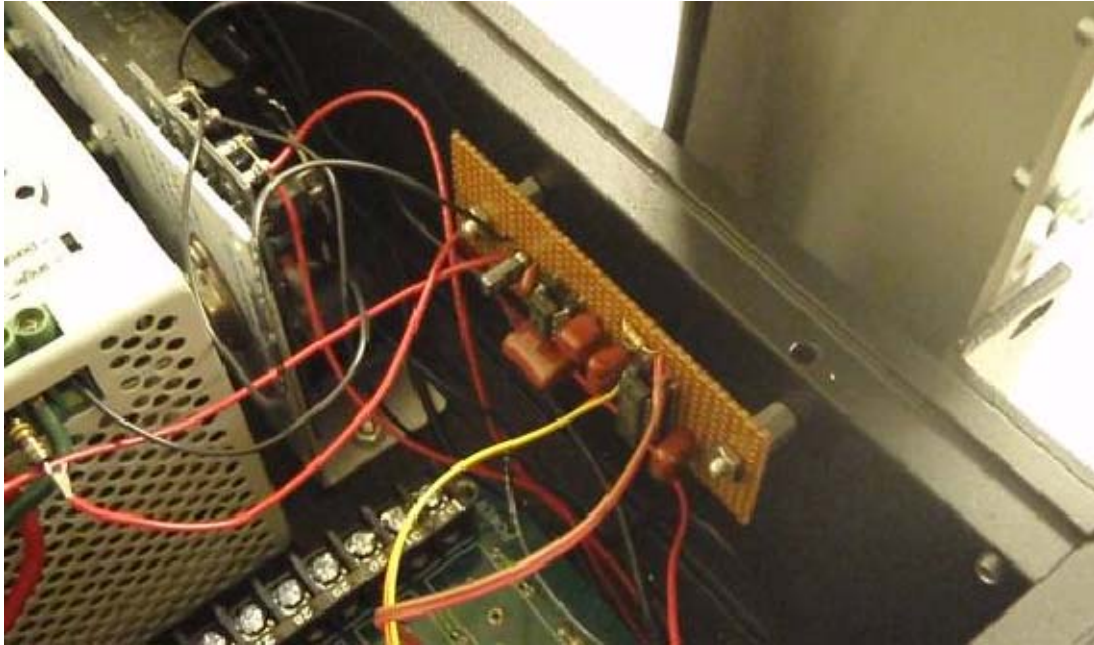
Figure 18.   Fuel Injector's Pulse Generator

Figure 19.   CRYDOM Solid-state Relay D1D40

Beside the fuel injector, the control system also centralizes control for the electro-pneumatic valves controlling the flow of air, fuel and nitrogen into the combustion chamber. The solenoid valves (Swagelock SS-43GS6-33C and SS-43GS4-31C) are electrically wired and controlled by CRYDOM solid-state relays 6321 (refer to Figure 20). The three 24VDC power supplies (Carlo Gavazzi SPD242401(B) 24V) power these. The 24VDC power supplies (refer to Figure 21) are connected in parallel to also provide the essential start-up current for the fuel injector.

Figure 20.   CRYDOM Solid State Relays 6321
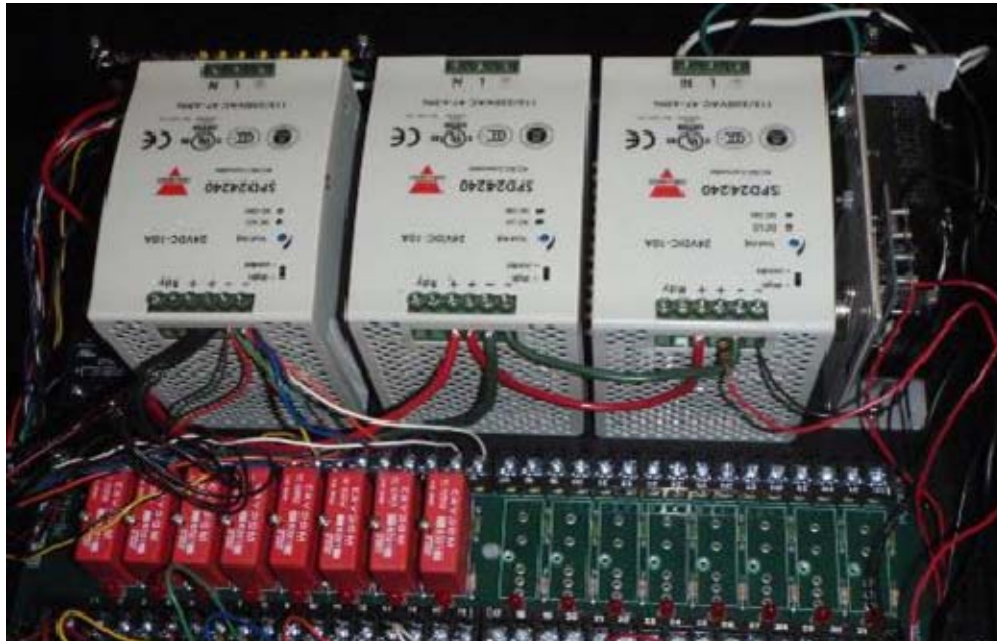
Figure 21.   Carlo Gavazzi SPD242401(B)24V

4.   The Supply System

The supply system (Figure 22) has two fuel tanks installed vertically. These are 150 mL high-pressure cylinders (Swagelock 316L-50DF4-150). The main purpose for having two fuel tanks is to allow a quick changeover from a baseline fuel test to a bio-fuel test (refer to Figure 23). By means of the hand valves, the cylinders can be isolated and/or removed from the supply system for refill or maintenance. Rupture Discs are used for prevention of overpressure (refer to Figure 24). The supply system also consists of a pressurized nitrogen tank and a compressed air tank (see Figure 25).
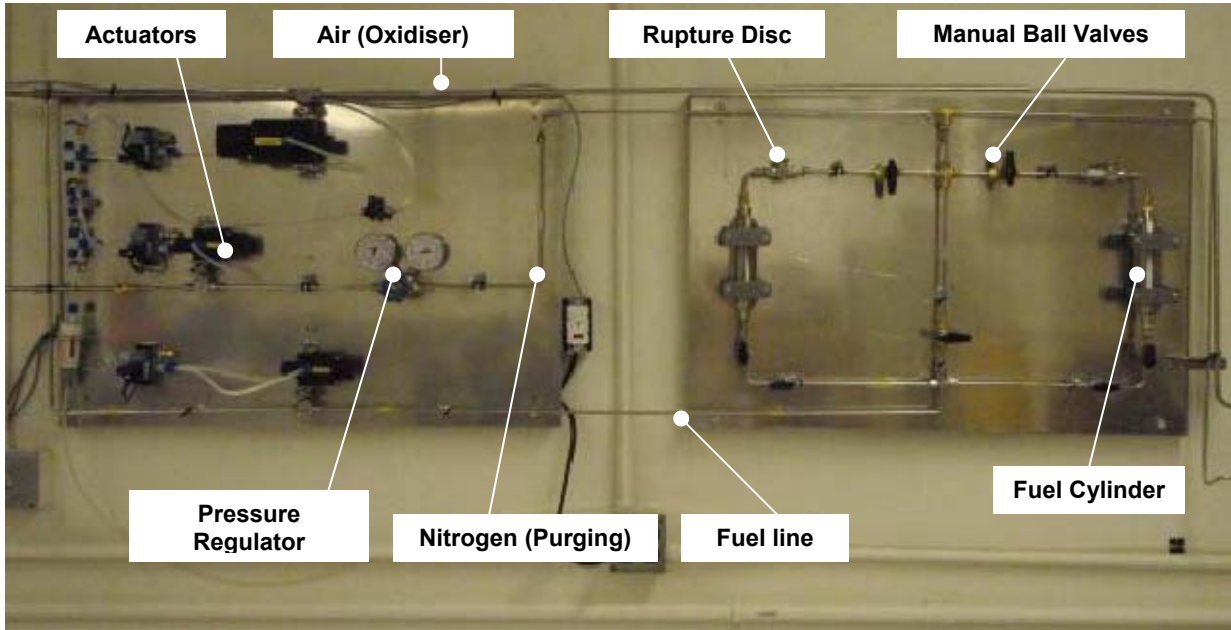
Figure 22.   The Supply System
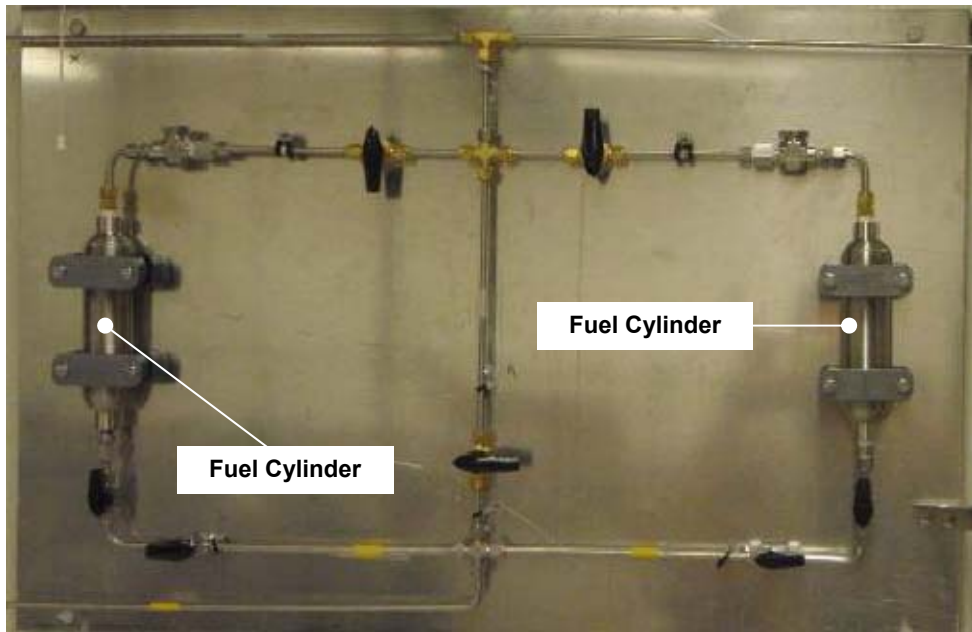
Figure 23.   Fuel Cylinders
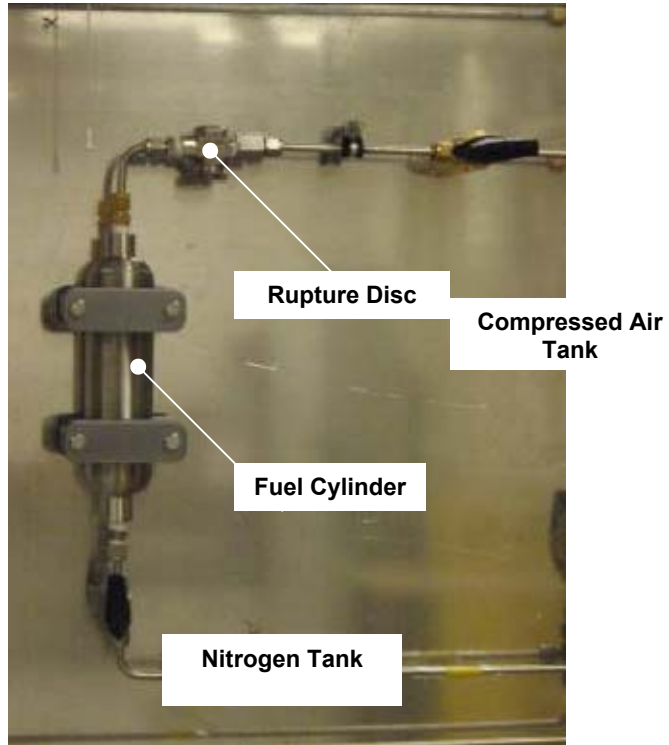
Figure 24.   Fuel Cylinder Attached to Rupture Discs and Ball Valves
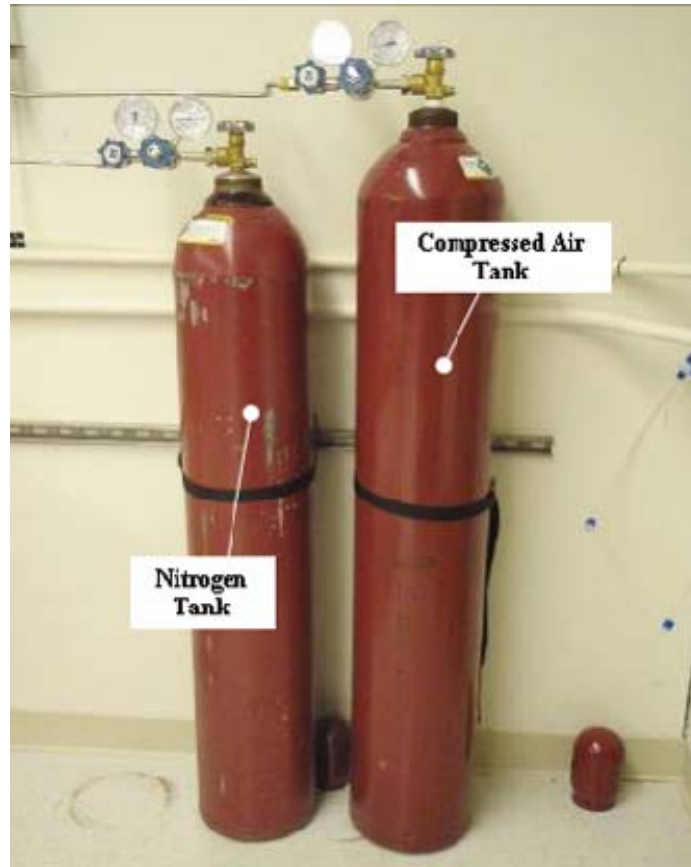
Figure 25.   Nitrogen and Compressed Air Tank

The electro-pneumatic ball valves (Swagelock SS-43GS6-33C and SS-43GS4-31C) are used to control the flow of air (oxidizer), nitrogen (purging gas) and fuel into the combustion chamber (refer to Figure 26). A regulator (Matheson-tri-gas 3040-CGA-580) can deliver air pressure from 100 to 2500 psig This is also used to control the pressure and flow rate of air mixing with fuel for combustion.
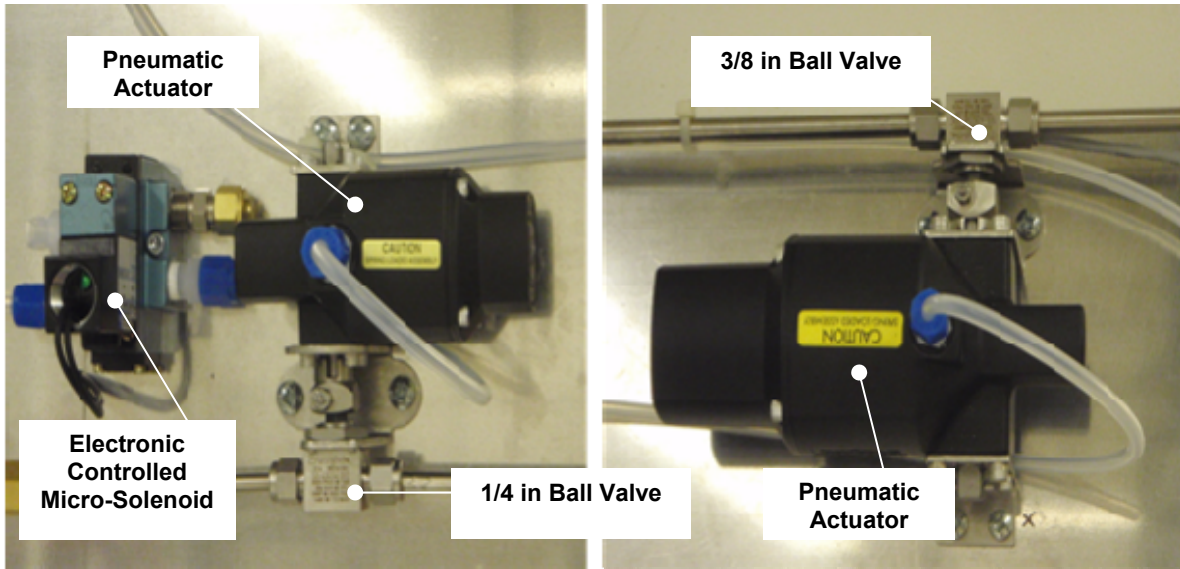
Figure 26.   Swagelok Electro-pneumatic Ball Valves

The control system is also comprised of Swagelok ball valves (refer to Figure 27). These are used to control the desired flow of air and fuel into the combustion chamber. Two regulators (Matheson-tri-gas 3020-CGA-590) with delivery pressure 20 to 500 psig regulate both the compressed air and nitrogen into the combustion chamber.
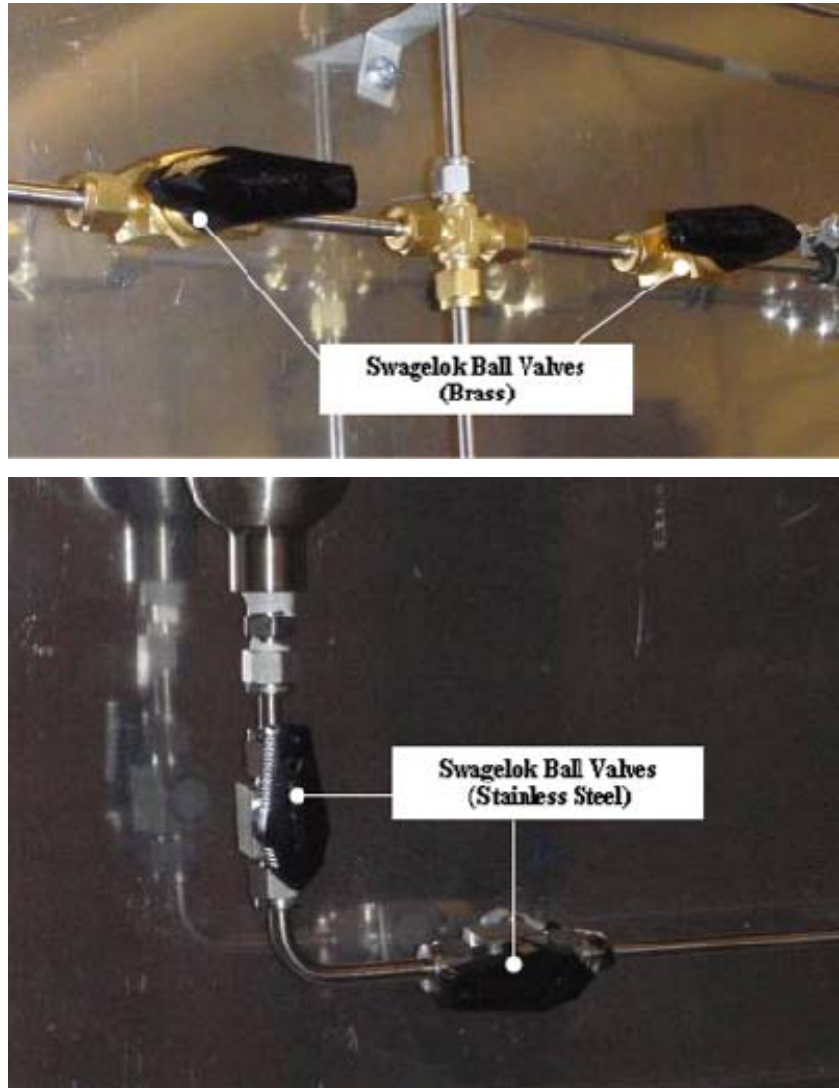
Figure 27.   Swagelok Steel Ball Valves (Brass and Stainless)

D.   FUNCTIONAL CHECKS AND CALIBRATIONS

1.   Leak Test for Tubing and Piping Systems

Bubble testing, which does not require high sensitivity, is the methodology employed. Liquid leak detector (Swagelok MS-Snoop-8OZ), a liquid soapy solution, was applied at the tube/pipe fittings followed by pressurizing these systems so that any emergence of bubbles will indicate a leak. The leak tests (Figure 28) were conducted initially using shop-air (90 psig). Once these leaks

were corrected, a final test took place at high pressure using compressed air (up to 1,500 psig for the fuel lines and up to 500 psig for the air and nitrogen purge lines).
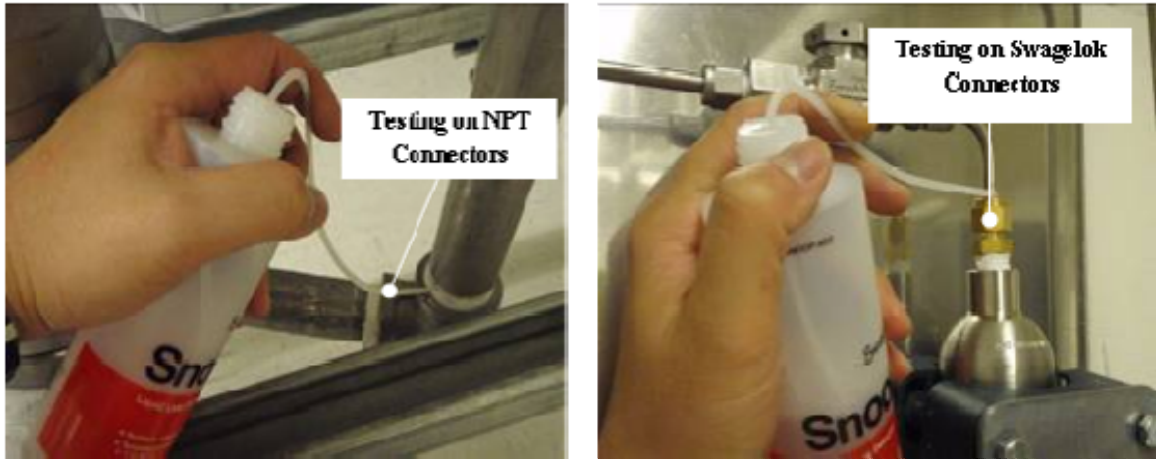
Figure 28.   Leak Test Conducted on Tube and Pipe Fittings.

2.   Leak Test for Combustion Chamber

Similar bubble testing methodology was employed for the leak test of the combustion chamber. Soaping liquids were applied at all the ports and flanges. The chamber was then pressurized. Any leaks found were corrected by either re-tightening or by adding pipe thread compound rather than utilizing Teflon tape.

3.   Calibration of High Speed Detectors

An enclosure (Figure 29) is designed and fabricated to house the detector at one side and a light source on the opposite side. To measure the signal of the detected light source, the detector is connected to an oscilloscope. The detector is then calibrated to the required sensitivity to detect flame wave in combustion chamber for experimentation. Figure 30 depicts the oscilloscope signal reading during the calibration of the detector.
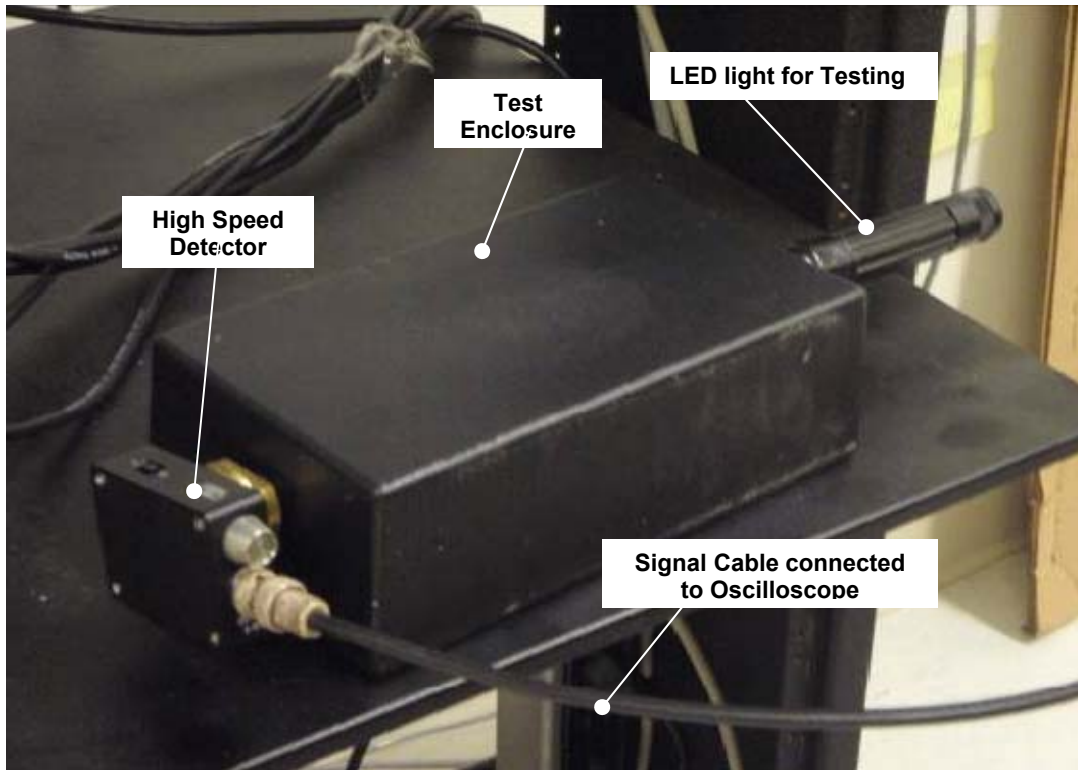
Figure 29.   Detector Connected to Test Enclosure for Measurement by Oscilloscope

Figure 30.   Signal Reading from Oscilloscope during Testing

4.   Spark Test for Igniters

Inside the combustion chamber (Figure 31), the electrodes are set at the required separation and the circuitry is closed to generate the required sparks. The spark electrodes were machined from tungsten and mounted on the wall of the combustion chamber by means of NPT-threaded mounted nuts. These were machined from Teflon material to provide electrical isolation from the combustor chamber. The electrodes are wired to a circuit with a piezoelectric igniter (Figure 32) for release of charges when required to create sparks required for combustion in the chamber. Prior to conducting experiments, spark test are sufficiently performed by visual inspection.
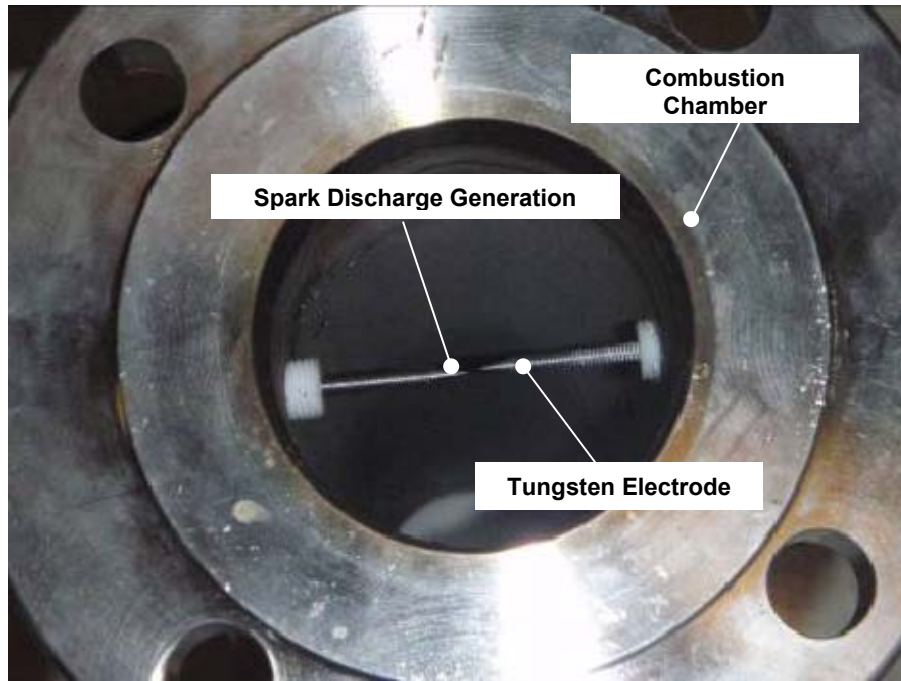
Figure 31.   Electrodes Depicting Spark Gap Setting for a Healthy Ignition Event.

Figure 32.   Piezoelectric Igniter used for the Generation of Sparks

5. Functional Check for Electro-pneumatic Actuators

The functionality of these actuators, as shown in Figure 33, open and close ball valves in the various gaseous or fuel supply systems. They are tested by switching levers at the control system to ensure that the micro-solenoids are actually opening and closing. This allows the shop air to engage or disengage the actuators, which, in turn, open or close the ball valves.
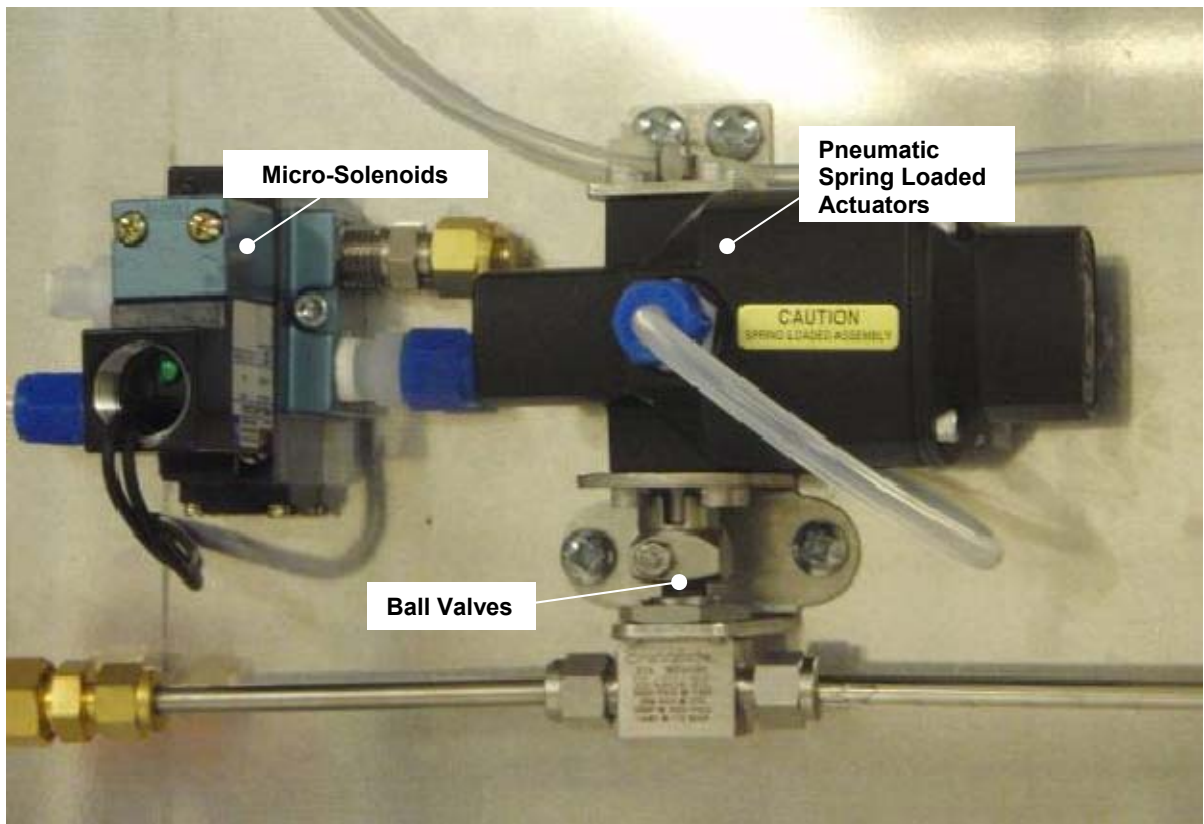
Figure 33.   Activation of Electro-pneumatically controlled Ball Valves

6. Functional Check for Manual Hand Valves

To either allow or stop flow within the Swagelok tubing, all the ball valves are checked by means of knob turning

E. INSTRUMENTATION AND MEASUREMENT

1. Determination of Volumetric and Mass Flow Rate for Fuel Injector

A stainless steel chamber with a manual valve at the bottom is fabricated to measure the volumetric flow rate of the fuel injector. The former is attached to the top flange of the combustion chamber (refer to Figure 34). Fuel is delivered to the fuel injector at a prescribed pressure (from 100 to up to 1,500 psig). The fuel injector is activated and the fuel is sprayed and collected in the chamber. Once the fuel supply is cut off, the system is allowed to settle for about 1 minute before the fuel is collected into a graduated beaker by simply opening the ball valve.
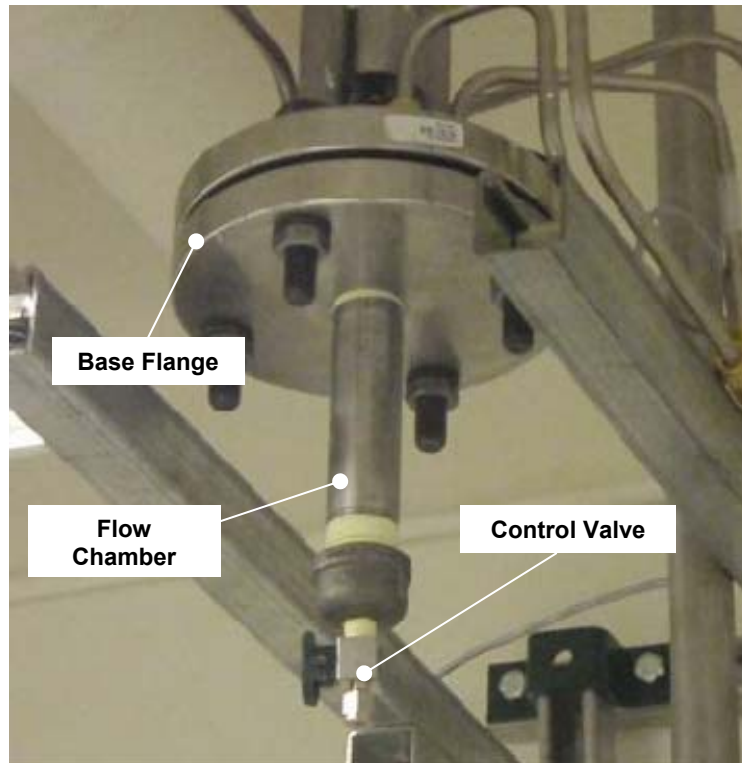
Figure 34.   Measuring (Flow Rate) Device attached to the Combustion Chamber for Measurement of Volumetric Flow Rate of Fuel Injector
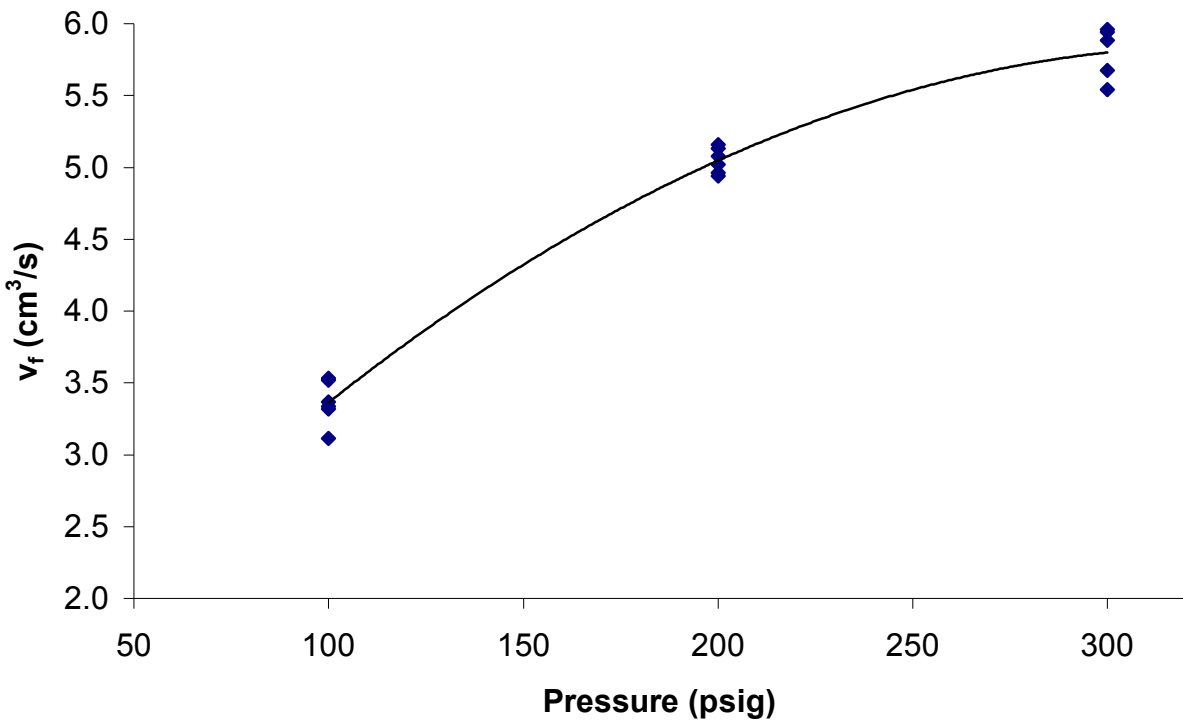
Figure 35.   Graph of Flow Rate for Fuel Injector versus Pressure

Similar tests are repeated for various pressure settings and a graph (Volumetric Flow rate vs. Pressure) is generated for the used fuel injector. For a given fuel, with its known density, the mass flow rate for the former can be determined from the obtained graph shown in Figure 35.
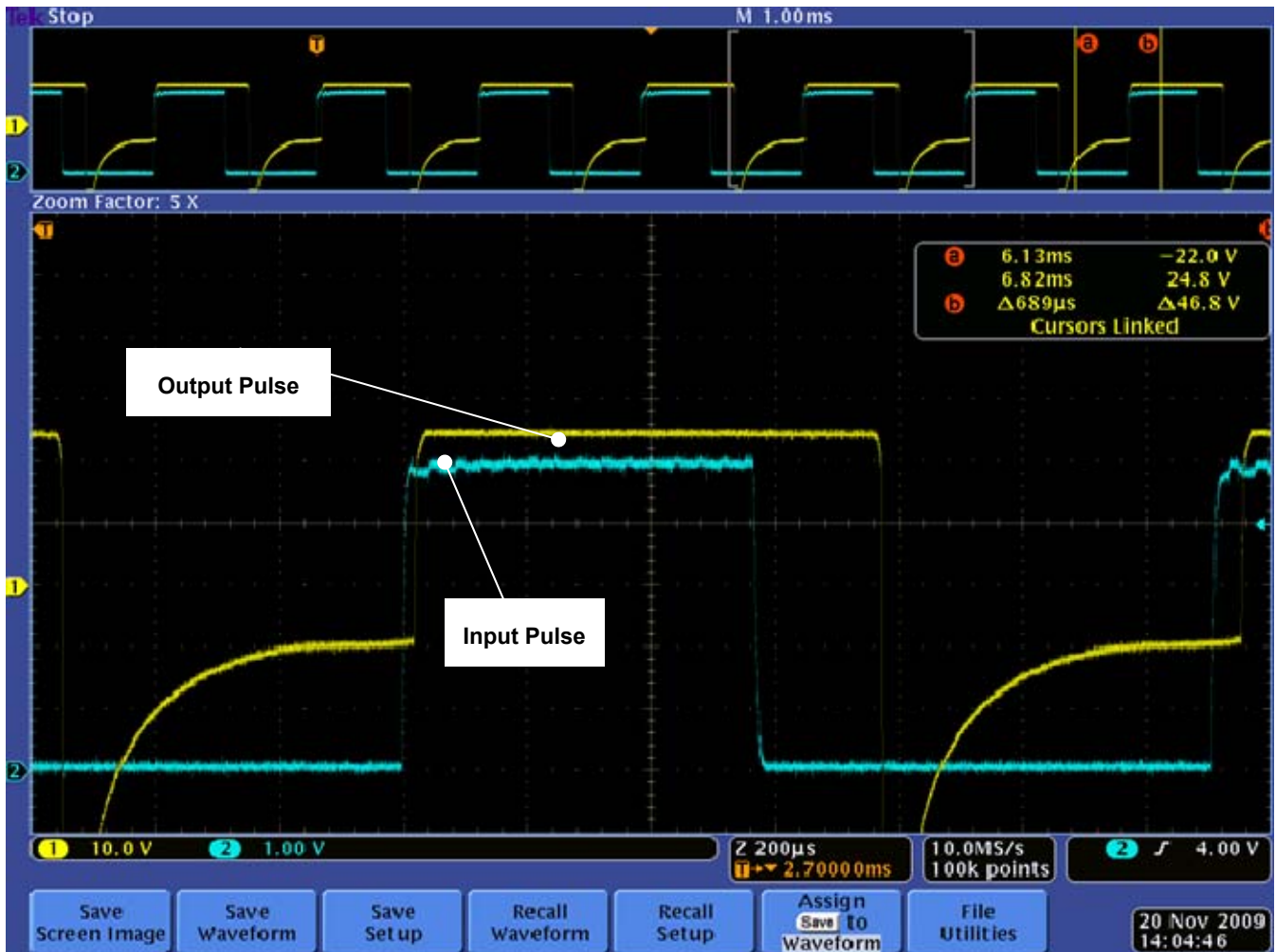
Figure 36.   Input and Output Pulses

A set of pre-determined pulse lengths (varying from 1 to 10 sec) is used to estimate average and transient flow rates. The input pulse (5VDC) was set at ON-Time of 575 µs and a Cycle Time of 1.32 ms. The output pulse from the CRYDOM relay to Injector (24 VDC) was measured to have an ON-Time of 719 µs and a Cycle Time of 1.29 ms. Refer to Figure 36 for the input and output pulses.

2. Measurement of Test Conditions

Pressure, temperature and humidity are recorded for the day when the experiment is conducted in the laboratory.

3. Determination of Flame Speed

High Speed Detectors (Thorlabs DET36A) are connected to the combustion chamber at known separations (10 cm from the centre of hole to the other centre of hole). Each detector has a photodiode and internal 12V bias battery enclosed in rugged aluminum housing. Housings made of brass material are fabricated to mount the detectors vertically on the wall of the combustion chamber. The fuel and air mixture upon ignition by the spark discharge will initiate combustion and generate a flame wave propagating vertically downwards along the inner side of combustion chamber. The detectors will detect these flame waves and the detected signals are then relayed to an oscilloscope where the time of arrival of the waves is determined. With known distances between each peak the flame speed can then be determined.

III.   RESULTS AND ANALYSIS

A.   DETERMINATION OF LAMINAR FLAME SPEED

The flame velocity, which is also known as the laminar flame speed, can be defined as the velocity at which unburned gases move through the combustion wave in the direction normal to the propagating wave surface. In the experimental setting, the laminar flame flow field within the combustion chamber is measured using the high-speed detectors. The detectors detect these flame waves and the detected signals are then relayed to an oscilloscope where the time of arrival of the waves was determined. The flame speed can thus be determined with the known distances between each peak.

Prior to the conduct of any flame speed measurement, there is a need to establish the flow rate of fuel and air flowing into the combustion chamber. The mass flow rate of fuel can be obtained from the experimental measured volumetric flow rate and the known density of fuel. Both the volumetric and mass flow rate of air can be determined based on the derived stoichiometric equation and the known density of air. The time required to fill combustion chamber can also be determined from the calculated volume of combustion chamber and the measured volumetric flow rate of both fuel and air at various pressure settings.

B.   DETERMINATION OF FUEL TO AIR RATIO

Kerosene, with an average chemical composition equivalent to $C_{12}H_{26}$, is used for the determination of mass flow rate of the fuel injector. Under stoichiometric conditions, the complete combustion of kerosene with air (oxidizer) yields

$$C_{12}H_{26} + 18.5(O_2 + 3.76N_2) \rightarrow 12CO_2 + 13H_2O + 69.56N_2$$
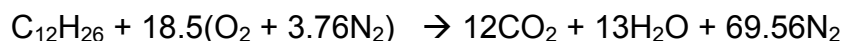
assuming stoichiometric condition occurs at complete combustion;

equivalence Ratio (Φ) = $\dfrac{\textit{fuel to air ratio}}{\textit{fuel to air ratio (stiochiometric)}}$

From the combustion equation, the fuel to air ratio (stoichiometric) can be computed as follows

$$\left.\frac{Fuel}{Air}\right|_{S} = \frac{(12\times \text{ Mass Weight of Carbon}) + \left(26\times \text{ Mass Weight of Hydrogen}\right)}{\left(18.5 \times \text{Mass Weight of Oxygen} + 69.56\times \text{ Mass Weight of Nitrogen}\right)}$$

= 0.06693

for stoichiometric condition, ϕ = 1;

Thus, the fuel to air ratio can be computed as $\left.\dfrac{Fuel}{Air}\right|_{S}$ = 0.06693.

C.   DETERMINATION OF MASS FLOW RATE OF FUEL ($_{FUEL}$)

From the relationship of the fuel to air ratio obtained, the mass flow rate of air can be computed once the mass flow rate of fuel is determined. To determine the mass flow rate of fuel, the volumetric flow rate of fuel can be measured experimentally as a function of pressure. The mass flow rate can then be obtained by multiplying the density of fuel to the measured volumetric flow rate of fuel.

The volumetric flow rates of fuel were measured experimentally as a function of pressure. Two sets of data were collected at each pressure (for pressure at 50, 75, 100, 200 and 300 psi). The fuel injector was turned on for 5 sec and 10 sec, respectively, and the amount of fuel dispensed was collected and measured. The volumetric flow rate of fuel is obtained by dividing the measured volume of fuel over the time duration at each respective pressure. A graph of volumetric flow rate of fuel as a function of pressure is plotted in Figure 37.
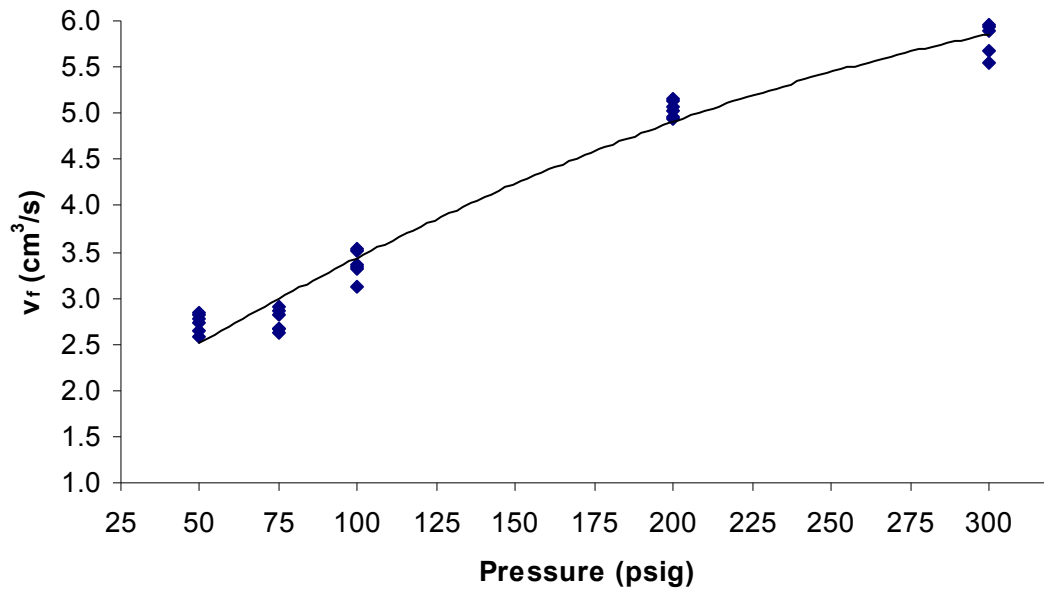
Figure 37.   Volumetric Flow Rate of Fuel vs. Pressure

The mass flow rate of fuel can, thus, be obtained by multiplying the known density of fuel to the measured volumetric flow rate of fuel. Refer to Figure 38 for the graph of mass flow rate of fuel as a function of pressure.
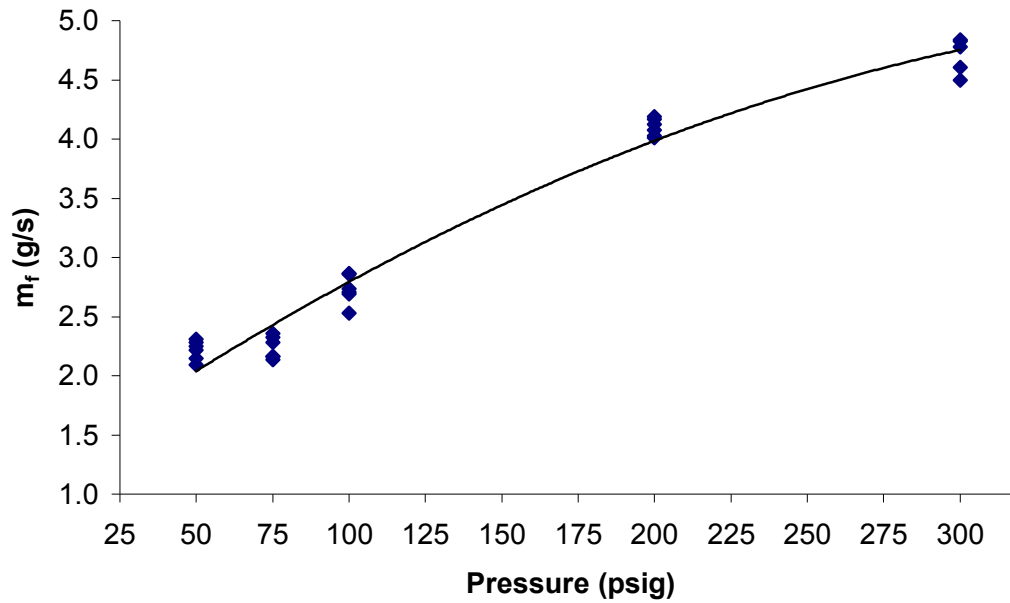
Figure 38.   Mass Flow Rate of Fuel vs. Pressure

D.   DETERMINATION OF MASS FLOW RATE OF AIR ($\dot{m}_{AIR}$)

equivalence ratio (Φ) = $\dfrac{fuel\ to\ air\ ratio}{fuel\ to\ air\ ratio\ (stiochiometric)}$

re-arranging the equation in terms of mass flow rate of air ($\dot{m}_{air}$) yields

$$\dot{m}_{air} = \frac{\dot{m}_{fuel}}{\left.\frac{fuel}{air}\right|_{S}} \times \frac{1}{\phi}$$

for stoichiometric condition, $\phi = 1$

fuel to air ratio can be computed as $\left.\dfrac{fuel}{air}\right|_{S} = 0.06693$.

The mass flow rate of air can thus be calculated for the corresponding mass flow rate of fuel at various pressure settings. The graph of mass flow rate of air as a function of upstream pressure for d = 0.137 in choke is depicted in Figure 39.
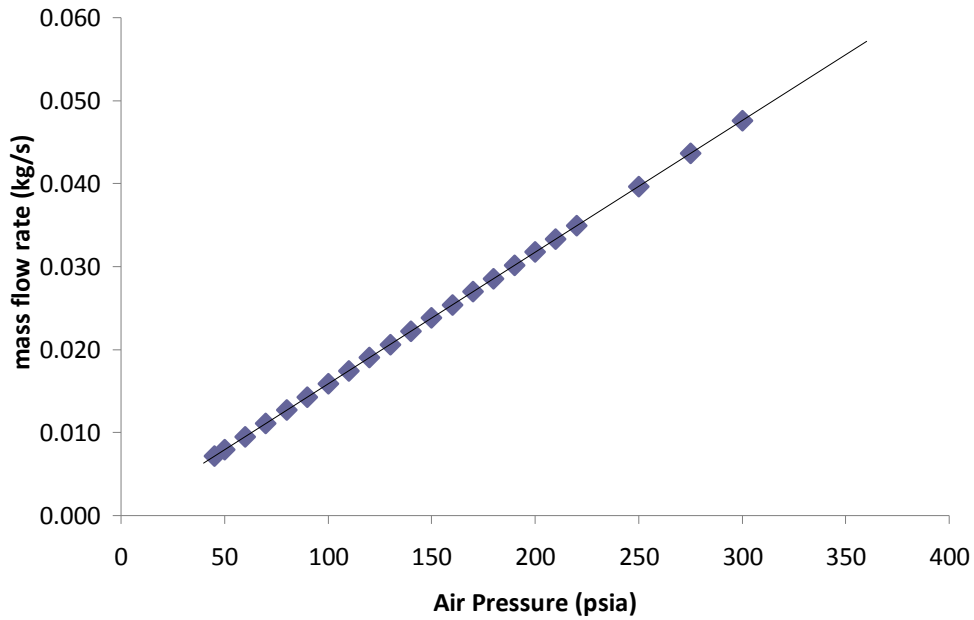
Figure 39.   Mass Flow Rate of Air vs. Pressure

Figure 40 depicts the relationship of mass flow rate of air ($\dot{m}_{air}$) vs. equivalence ratio (Φ) at the pressure of 100, 200 and 300 psi.
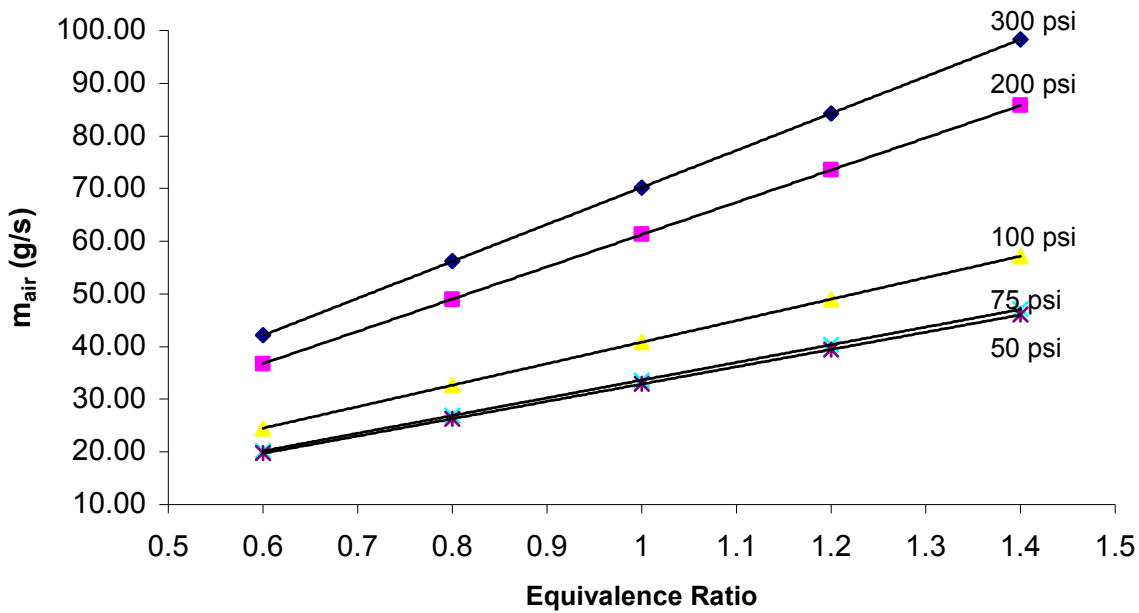
Figure 40.   Mass Flow Rate of Air vs. Equivalence Ratio for various Fuel Pressure Settings.

Once the required mass flow rate of air is determined, suitable choked orifice can then be selected. This controls the appropriate flow rate of air into the combustion chamber required to conduct the flame speed test at various pressure setting.

E.   CALCULATION OF TIMING REQUIRED TO FILL COMBUSTION CHAMBER

Based on the dimension of the test rig, the volume of the combustion chamber can be computed as follows

$$vol = \frac{\pi \, d^2}{4} \times l$$

where diameter of chamber (d) = 0.075 m and length of chamber (l) = 1.83m.

52

Thus, the volume of combustion chamber is calculated as 0.0081 m^3. The required time for air and fuel to fill the combustion chamber is governed by the equation as follows

$$Time \text{ required} = \frac{vol \text{ of combustion chamber}}{volumetric \text{ flow rate}}$$

Based on the density of fuel as 810 kg/m^3 and the density of air as 1.204 kg/m^3, the timing for fuel and air to fill the combustion chamber is tabulated in Table 2.

F.   MEASUREMENT OF LAMINAR FLAME SPEED

The desired equivalence ratio (Φ) is attained by the appropriate control of mass flow rate of fuel into the injector and mass flow rate of air into the combustion chamber. Upon spark ignition, flame waves propagate down the combustion chamber. The high-speed detectors detect these passing flame waves and relay the signals to an oscilloscope where the time of arrival of the waves is determined. The flame speed can thus be determined with the known distances between each peak.

$$S_L = \frac{\Delta y}{\Delta t}$$

where S_L = laminar flame speed

Δy = distance between the detectors

Δt = time difference

G.   IGNITION AND FUELING COMPLICATIONS

During dry air testing, the piezoelectric igniter employed to generate the required spark arc for combustion was observed to be performing well. There was constant spark arc generated for every depression on the spring activator of the igniter. However, during the actual experimentation, when fuel was injected

into the Combustion Chamber, the igniter was not working up to expectation. There were times where no spark arc was produced.

The selection criterion for the fuel injector was primarily based on its dispersion fuel droplet size. It was only realized at the testing stage that the injector has unexpectly large flow rate, which induced large amount of impingment onto the walls of the Combustion Chamber. This may have skewed the local fuel-air ratio to leaner values than anticipated on the center axis of the Chamber and much richer fuel-air ratios near the wall. A more detailed feasibility study on the compatibility between the fuel flow rate and the current test rig may be required.

IV. CONCLUSIONS

Bio-diesel is definitely a promising alternative to petroleum-based diesel fuels. This is primarily because of its ability to reduce unwanted emissions in combustion engines. The ease of production of bio-diesel through growth of plants and algae as well as livestock has also made it a great potential to supplant a fraction of petroleum-based fuels.

The experiments conducted served as an exciting step towards the original objectives and goals. Because of many obstacles in the experiments, much important knowledge was gained which lays the foundation for future research.

A laboratory-based test rig was designed and fabricated with the intention to directly measure the laminar flame speed of bio-diesel. For the initial phase of the design, the mass flow rate of fuel (into the fuel injector) and the mass flow rate of air (into the combustion chamber) required sizing the choked orifice. Kerosene was utilized as the testing fuel. Controlling the fuel flow rate into the injector and the air flow rate into the combustion chamber was recognised as a crucial parameter. This is because it effects the accuracy and the conditions, i.e., fuel-lean or fuel-rich. This is where the laminar flame data is obtained.

Critical ignition and fueling issues, however, were uncovered during experimentation. The current ignition system employing the piezoelectric igniter to generate the required spark arc for combustion was found to be unreliable. There were times where no spark arc was produced. For future research, it is highly recommended to, rather than using the current piezoelectric igniter, use a capacitive discharge system. This would generate a more reliable and stronger spark arc, which is mandatory for combustion.

In addition, the study's experiments strongly indicated that, prior to future research, it would be necessary to re-evaluate the compatibility between the fuel flow rate and the current test rig. This will require a detailed feasibility study on the current fuel injector.

After analyzing the experiments, along with the important obstacles and knowledge gained from them, the next section provides suggested improvement pathways to the current design. This will pave the way towards successful solutions, which means obtaining the original experimental objectives and goals.

V.   RECOMMENDATIONS

A.   INCLUSION OF FUEL AND AIR PRE-HEAT SYSTEM

The inclusion of a pre-heat system for fuel and air prior injecting and mixing in the combustion chamber would alleviate the need for small droplet size diameters as per D^2 law, described in the earlier section. This will thus allow the usage of wider range of fuel injectors with larger D_{32s} but with a more appropriate flow rate.

B.   IMPLEMENTATION OF LABVIEW

For better integration, accessibility and control of both the instrumentation and measurement hardware, it is recommended to include a control-programming environment such as LabVIEW to integrate measurement, test, and control systems of the test rig. LabVIEW offers integration with hardware devices and provides a good spread of already built-in libraries for advanced analysis and data visualization.

C.   PROVISION FOR OPTICAL ACCESS

For future experiment, it will be good if the research can be expanded to the study of the formation of flame. An optical moderate-pressure chamber is thus desirable. The upgrade will serve as a tool for on-site observation of dynamic changes of flame formation within the combustion chamber. The current test rig caters the possibility for such modular modifications to be implemented for future improvement. Flame thickness can then be observed and computed and the relationship between flame thickness and equivalence ratio can be established. Reaction zone area of the flame can also be observed and high-speed video can be used as another possible mean to determine flame speed.

D.   SPECTROSCOPIC MEASUREMENT

Spectroscopy instruments may also be included in future testing to measure the chemical composition and physical properties of the bio-fuel. During the design phase, the combustion chamber has already factor in such requirement to allow for future installation if required.

APPENDIX

EXPERIMENTAL PROCEDURES

Pre-experimental checks are required prior the conduct of actual experiment. The procedures for the pre-experimental functional checks are depicted as follows:

1.   Power-up the control system (by pulling up the switch) to ensure its functionality prior to performing checks on other sub-components. The red bulb at the top right corner of the control panel should be lilted to indicate that the control system is functioning.

2.   Remove the top modular of the combustion chamber to conduct functional check for *Injector* and *Spark Plugs*.

3.   Conduct functionality check for the injector at the top-flange by activation of the lever at the control panel to close the circuitry and observe for pressure blowout from the injector. The injector should generate a "ooze" sound, discharging small amount of fuel. Place a container underneath the injector to trap these residues during the conduct of functional check. Igniter nozzle tip inspections will be performed at the end of each test phase to ensure no coking occurred during the test burns.

4.   Ensure that the tungsten tips of the spark plugs are placed in accordance to the required separations. Turn on the lever at the control panel to close the circuitry and observe for spark generation. Adjust the separation of the tungsten tips by clockwise or anti clockwise turning to obtain the desired spark generation. Once the check for the spark generation is completed, the top

modular is mounted back to the main combustion chamber and sealed with the top flange by means of sealing gasket. For every 20 firings, the tungsten tips' separation must be checked and adjusted if required to ensure sufficient spark generation during conduct of subsequent flame speed experiments.

5.   Conduct check on the piezoelectric igniter by depressing the knob actuator. Ensure that sparks are generated between the tungsten sparks plugs for every depression.

6.   Turn on the valve for compressed air to allow the electro-pneumatic actuators to be pressurized.

7.   Flip on/off the individual switches at the control panel and observe the opening/closing of the actuators.

8.   Ensure all manual valves can operate in both open and close positions. Place them all in close positions prior the commencement of experiment.

9.   Ensure that the high-speed detectors are in their correct positions on the combustion chamber and that they are properly connected to the oscilloscope.

10.   Ensure that the wall exhaust fan is in working condition.

11.   Complete all pre-experimental functional checks for injector, spark plugs, solenoid valves, manual valves, high-speed detectors and exhaust fan prior mounting of the alcohol and fuel cylinders to the supply system.

12.   Fill fuel into the respective cylinders and connect them to the supply system. Check for leakages and ensure that the top and bottom connectors of the cylinders are tightly sealed by Teflon tape.

13.   Perform diligent check at the connectors near the mounting area of the alcohol and fuel cylinders and ensure that all connectors are properly sealed (by pipe thread tape).

The following schematic diagram of the test system is stipulated for reference in the subsequent elaboration of the experimental procedures.
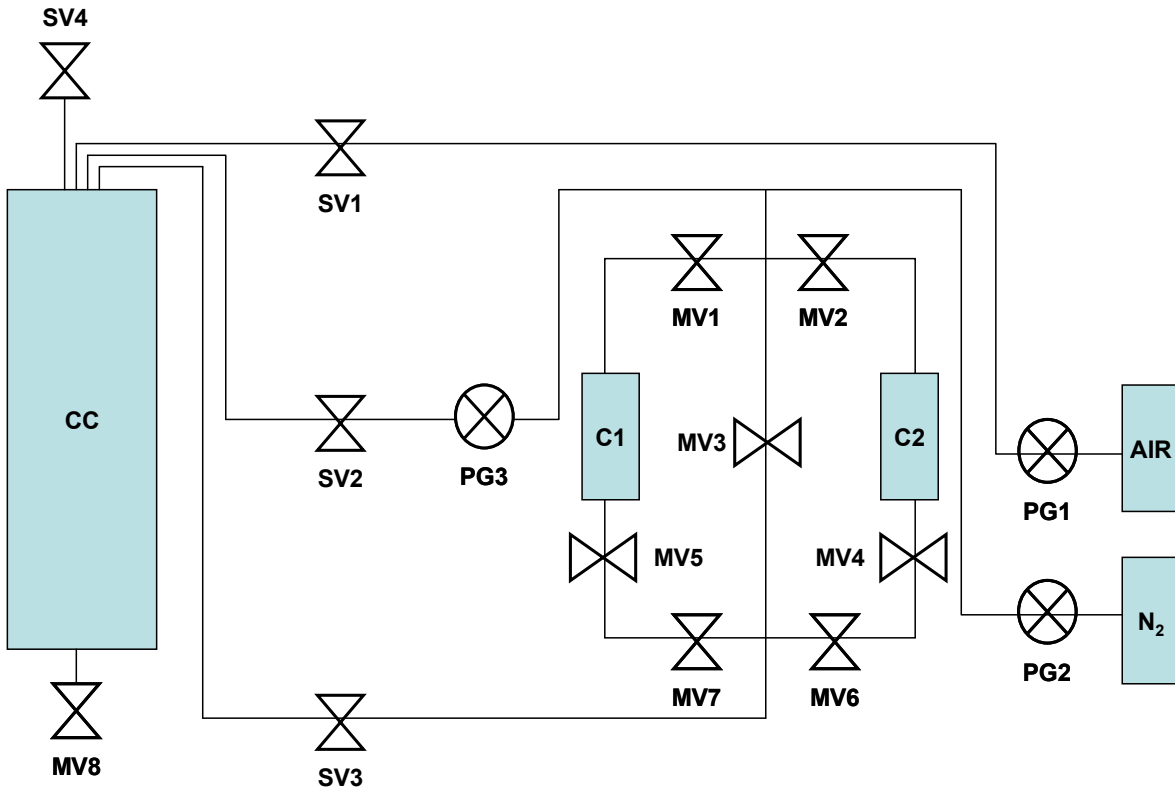

Figure 41.   Schematic Diagram of the Test Rig

Reference Figure 41 for the following:

PG1 regulates pressure into the combustion chamber and PG2 regulates pressure into both combustion chamber and supply system. The series of manual valves (MV1 to MV7) controls the fuel flow from fuel cylinders (C1 and C2). PG3 regulates the pressure of nitrogen required for purging of the combustion chamber. The solenoid valves, SV1 and SV2, control the flow gateway for air (oxidizers) and nitrogen (purging gas) into the combustion chamber, respectively. SV3 controls the fuel supply into the combustion chamber. Both SV4 and MV8 control the release of pressure in the combustion chamber to the exhaust wall fan.

The experimental procedures for the conduct of the ***Fuel Injector Flow Rate Characterization***, ***Flame Speed Determination***, ***Purging*** and the ***Shutdown*** are stipulated as follows:

1.   Procedures for fuel injector flow rate characterization:

    a.   Turn on wall fan (to Speed 1) for ventilation prior the conduct of experiment.

    b.   Verify all Swagelok and NPT connections are properly sealed.

    c.   Connect Channel 2 of the oscilloscope to the input of D1D40 CRYDOM Relay. Connect Channel 1 of the oscilloscope to a 50 ohms terminal to the injector output terminal located behind the control box.

    d.   Fill the fuel cylinder with the desired fuel for testing.

e. Pressurize system to initial set pressure (i.e., 100 to 500 psig).

   i. Verify only the fuel tank in use is pressurized (i.e., open only the appropriate manual ball valves and ensure all the remaining manual ball valves are at closed position).

   ii. Ensure all levers at the control box are at closed position prior to powering up the control box.

   iii. Ensure that the shop sir valve is turn on.

   iv. Open SV3 by flipping up Lever 3 at the control box. This will enable fuel flow from fuel cylinder to injector.

   v. Ensure nitrogen purge regulator is set to zero at PG3.

   vi. Open the nitrogen regulator hand valve (i.e., with one full turn counter-clockwise) at PG2.

   vii. Open the main valve of the nitrogen tank and verify that the supply pressure is sufficient.

   viii. Set test rig to desired pressure level by turning the nitrogen regulator hand valve at PG2.

   ix. Perform visual inspection to test rig to ensure no leaks.

f. Perform fuel calibration at various set pressure. (i.e., 100 to 500 psig).

i. Flip up Lever 8 at the control box to activate the fuel injector and collect the dispensed fuel in the measuring device. Use a stopwatch to measure the time duration for fuel dispersal.

ii. Measure the collected fuel in graduated cylinder.

iii. Divide the volume of fuel collected by the time taken to obtain the volumetric flow rate.

iv. Multiple the volumetric flow rate to obtain the desired mass flow rate for fuel.

2. Procedures for flame speed determination:

a. Turn on wall fan (to Speed 1) for ventilation prior to conducting the experiment.

b. Verify all Swagelok and NPT connections are properly sealed.

c. Connect Channel 1 and 2 of the oscilloscope to the output of High Speed Detectors. Ensure connectivity of the High Speed Detectors to the oscilloscope.

d. Fill the fuel cylinder with the desired fuel for testing.

e. Pressurized system to initial set pressure (i.e., 100 to 500 psig).

i. Verify only the fuel tank in use is pressurized (i.e., open only the appropriate manual ball valves and ensure all the remaining manual ball valves are at closed position).

ii. Ensure all levers at the control box are at closed position prior to powering up the control box.

iii. Ensure that the shop sir valve is turn on.

iv. Open SV3 by turning up Lever 3 at the control box. This will enable fuel flow from fuel cylinder to injector.

v. Ensure nitrogen purge regulator is set to zero at PG3.

vi. Open the nitrogen regulator hand valve (i.e., with one full turn counter-clockwise) at PG2.

vii. Open the main valve of the nitrogen tank and verify that the supply pressure is sufficient.

viii. Set test rig to desired pressure level by turning the nitrogen regulator hand valve at PG2.

ix. Perform visual inspection to test rig to ensure no leaks.

f. Perform flame speed test at various set pressure.

i. Flip up Lever 8 at the control box to activate the fuel injector. Use a stopwatch to measure the time duration for fuel dispersal.

66

ii. Flip down Lever 8 to close the fuel injector. Allow a residue time of one minute before activating the spark electrodes.

iii. Depress the button of the piezoelectric igniter to activate spark generation in the combustion chamber.

iv. Observe the signals (at the oscilloscope) captured by the high-speed detectors. Record the delta time between Channel 1 and 2.

v. Divide the known separation distance between the high-speed detectors with the delta time to obtain the speed of flame.

3. Procedures for system purging:

a. Decrease the pressure from the nitrogen tank (PG2).

b. Turn on SV4.

c. Turn on SV2.

d. Turn on PG3 to slowly release pressure into the combustion chamber.

4. Procedures for system shut down:

a. Decrease the pressure from the nitrogen tank (PG2) and close the valve PG2.

b.   Turn on SV2.

c.   Increase the pressure from PG3 slowly to release pressure into the supply system.

d.   Close PG3 after pressure from supply system has been released.

e.   Close SV2.

f.   Ensure all MVs are at closed position.

g.   Turn on SV4 to release pressure in the combustion chamber.

h.   Close SV4.

i.   Close SV3 to cut fuel supply into combustion chamber.

j.   Close SV1 to cut air supply into combustion chamber.

k.   Turn off power for control box.

l.   Maintain operation of wall exhaust fan for another 5 minutes to allow ventilation of remaining fuel fumes in the room before shutting it down.

LIST OF REFERENCES

[1]   A.T. Holley, Y. Dong, M.G. Andac, F.N. Egolfopoulos, Combust, Flame 144 (3) (2006), pp. 448–460.

[2]   T.G. Scholte and P.B. Vaags, "Burning velocities of mixtures of hydrogen, carbon monoxide, and methane with air," Combustion and Flame, vol. 3, pp. 511–524, 1959.

[3]   California Air Resources Board, Procedure for the Detailed Hydrocarbon Analysis of Gasolines by Single Column High Efficiency (Capillary) Column Gas Chromatography, SOP No. MLD 118, Rev. No. 1.1, 1997.

[4]   B.H. Chao, F.N. Egolfopoulos, C.K. Law, Combust, Flame 109 (4) (1997), pp. 620–638.

[5]   M. Nishioka, C.K. Law, T. Takeno, Combust, Flame, 104 (3) (1996), pp. 328–342.

[6]   G.E. Andrews and D. Bradley, "Determination of burning velocities – Critical review," Combustion and Flame, vol. 18, pp. 133–153, 1972.

[7]   C.M. Vagelopoulos and F.N. Egolfopoulos, "Laminar flame speeds and extinction strain rates of mixtures of carbon monoxide with hydrogen, methane, and air," Proceedings of the Combustion Institute, vol. 25, pp. 1317–1323, 1994.

[8]   T. Lieuwen, V. McDonell, E. Petersen, and D. Santavicca, "Fuel Flexibility Influences on Premixed Combustor Blowout, Flashback, Autoignition, and Stability," Journal of Engineering for Gas Turbines and Power, vol. 130, pp. 2008.

[9]   W.A. Strauss and R. Edse, "Burning velocity measurements by the constant pressure bomb method," Proceedings of the Combustion Institute, vol. 7, pp. 377–385, 1958.

[10]   V.S. Yumlu, "Prediction of burning velocities of carbon monoxide-hydrogen-air flames," Combustion and Flame, vol. 11, pp. 190–194, 1967.

[11]   M.I. Hassan, K.T. Aung, and G.M. Faeth, "Properties of laminar premixed CO/H2/air flames at various pressures," Journal of Propulsion and Power, vol. 13(2), pp. 239–245, 1997.

[12] W. Yuan, A.C. Hansen, and Q. Zhang, 2003b, Predicting the physical properties of biodiesel for 436 combustion modelling, T*rans. ASAE* 46(6), pp. 1487–1493.

[13] M.S. Graboski. and R. L. McCormick, 1998, Combustion of fat and vegetable oil derived fuels in diesel engines, Prog. Energy Combustion. Sci. 24(2), pp. 125–164.

[14] D. Singh, E. Croiset, P.L. Douglas, and M.A. Douglas, 2003, Techno-economic study of CO_2 capture from an existing coal-fired power plant: MEA scrubbing vs. O_2/CO_2 recycle combustion, pp. 102–20.

[15] M.E. Tat and J. H. Van Gerpen, 2000, The specific gravity of biodiesel and its blends with diesel fuel, J. American Oil Chem. Soc. 77(2), pp. 115–119.

[16] P.N. Giannelos, F. Zannikos, S. Stournas, E. Lois, and G. Anastopoulos, 2002, Tobacco seed oil as an alternative diesel fuel: Physical and chemical properties, Industrial Crops and Products, 16(1), pp. 1–9.

[17] R.L. McCormick, M.S. Graboski, A.M. Herring, and T.L. Alleman, 2001, Impact of biodiesel 414 source material and chemical structure on emissions of criteria pollutants from a 415 heavy-duty engine, *Environmental Science & Technology*, Vol. 35(9), pp. 1742–1747.

[18] V.L. Griend, M.E. Efldman, and C.L. Peterson, 1990, Modelling combustion of alternate fuels in a DI diesel engine using KIVA, Trans. ASAE 33(2), pp. 342–350.

[19] L.D. Clements, 1996, Blending rules for formulating biodiesel fuel, www.biodiesel.org/resources/reportsdatabase/reports/gen/19960101_gen-277.pdf. Accessed 3 Sep 2009.

[20] N.Y. Nsakala, G.N. Liljedahl, J. Marion, A.A. Levasseur, D. Turek, R. Chamberland, R. MacWhinnie, J.-X. Morin, and K. Cohen, 2004, Oxygen-fired circulating fluidized bed boilers for greenhouse gas emissions control and other applications, *Proceedings of Third Annual Conference on Carbon Sequestration, Alexandria, VA, USA.*

INITIAL DISTRIBUTION LIST

1. Defense Technical Information Center
   Ft. Belvoir, Virginia

2. Dudley Knox Library
   Naval Postgraduate School
   Monterey, California

3. Professor Jose O. Sinibaldi
   Naval Postgraduate School
   Monterey, California

4. Professor Knox T. Millsaps
   Naval Postgraduate School
   Monterey, California

5. Professor Yeo Tat Soon
   Director, Temasek Defence Systems Institute
   National University of Singapore

6. Tan Lai Poh (Ms)
   Director, Temasek Defence Systems Institute
   National University of Singapore